IDENTIFYING SOURCES OF GROUNDWATER RECHARGE IN ORAIBI WATERSHED, NAVAJO RESERVATION, ARIZONA: AN ISOTOPIC AND HYDROGEOLOGIC APPROACH

by

Derrick J. Slick

A Thesis

Submitted to the Faculty of Purdue University

In Partial Fulfillment of the Requirements for the degree of

Master of Science

Department of Earth, Atmospheric, and Planetary Sciences

West Lafayette, Indiana

May 2023

THE PURDUE UNIVERSITY GRADUATE SCHOOL
STATEMENT OF COMMITTEE APPROVAL

Dr. Lisa R. Welp, Chair

Department of Earth, Atmospheric and Planetary Sciences

Dr. Kenneth D. Ridgway

Department of Earth, Atmospheric and Planetary Sciences

Dr. Marty D. Frisbee

Department of Earth, Atmospheric and Planetary Sciences

Approved by:

Dr. Daniel J. Cziczo

ACKNOWLEDGMENTS

Contributions and support from many individuals helped make this thesis a rewarding experience. I thank my advisor, Dr. Ken Ridgway, for his guidance and scientific input during my graduate career. His focused insights, support, and enthusiasm in the field, classroom, and lab have helped me become a better scientist during my studies. I thank Dr. Lisa Welp (Purdue University) for helpful discussions as a chair committee member and for her guidance and support as my co-advisor. Her instruction in utilizing stable isotopes in my research especially prepared me for graduation and my future career. I also thank committee member Dr. Marty Frisbee (Purdue University) for providing me with helpful resources on the hydrogeology of the Southwest during my studies. He was especially important in helping me develop my research direction. I thank Dr. Christopher Andronicos (Purdue University) for insightful discussions and providing me with helpful resources and instruction on cross sections and geologic structures of the Southwest during my studies. I thank Ms. Janine M. Sparks (Purdue University) for guidance and support while I worked in the Stable Isotope Laboratory at Purdue University.

My collaborators were invaluable in collection of the datasets contained in this thesis. I thank Ms. Wai K. Allen and her family from Pinon, AZ for helping collect snow samples during the winter months. I thank Ms. Ann Romero of Black Mesa, AZ for allowing me to set-up a weather station near her house. I thank the Black Mesa community for their kindness and for letting me sample springs and wells within their customary use area. I also thank Navajo Nation Water Resource Department for their help and cooperation in providing me with well logs. I thank Dr. Crystal Cordova-Tulley for our discussions and providing me with precipitation collectors that provided vital datasets for my research.

Primary funding for this project was provided by the National Science Foundation Graduate Research Fellowship #2018269008. Additional funding and support were provided by the Department of Earth, Atmosphere, and Planetary Sciences, the Sloan Indigenous Graduate Program at Purdue University, the Hydrologist Helping Others Program funded by Dr. Lee C. Atkinson, and the Native American Educational and Cultural Center at Purdue University under the leadership of Ms. Felica Ahasteen-Bryant.

I am especially grateful for my friends in the Basin Analysis and Hydrogeology Groups for their informal reviews of my thesis, talks, and poster presentations. I also thank them for their support and sense of humor that made the occasional long days in the field and lab much easier.

Finally, I thank my family for their support and encouragement throughout the years that have helped me succeed in my academic endeavors.

TABLE OF CONTENTS

LIST OF TABLES

LIST OF FIGURES

ABSTRACT

Water is critical in the American arid southwest, including the Navajo Nation where groundwater supports livestock, farming, and the livelihoods of both Navajo and Hopi Tribal members. Groundwater availability is determined by precipitation and infiltration, and by geologic controls like fractures and permeability on recharge and permeability contrast in stratigraphy. This study aims to improve the understanding of surface-water and groundwater interactions in a single watershed known as Oraibi Wash. The Oraibi Watershed covers an area of 1,896 square kilometers and is a tributary to the Little Colorado River. For much of the southwestern U.S., there are two main ways groundwater is recharged; by rainfall and snowmelt. To help understand the recharge process, we integrate geologic analysis with stable water isotopes of δD and δ18O to identify sources of groundwater recharge along Oraibi Wash. In this study, I explored the geologic features associated with spring emergence. Strike and dip measurements were collected in the field and from previous studies of the Black Mesa Basin to construct a geologic cross section along Oraibi Wash. The cross section along with field observations identified both stratigraphically and structurally controlled springs. I also estimated the relative amounts of recharge supported by winter and monsoon seasonal precipitation using stable water isotopes. Springs and wells samples both clearly show the importance of winter precipitation recharge. Also springs that were stratigraphically controlled had a wider range in isotopic variability whereas structurally controlled springs had a narrower isotopic range. Implications for these new findings indicate that winter recharge of groundwater will be critical for Navajo communities along Oraibi Wash. Changes in precipitation due to climate change that impact winter precipitation will have profound effects on groundwater in Oraibi Wash, and consequently, also on the Native communities living along this drainage.

CHAPTER 1. INTRODUCTION

Oraibi Wash Site Description

The Oraibi Wash is a westward flowing drainage along Black Mesa and is one of the main tributaries of the Little Colorado River (Figure 1). The sustainability of groundwater resources is a critical concern in the Black Mesa Basin in northeastern Arizona. Black Mesa Basin (13,986 km^2) is the principal source of groundwater for the Hopi and Navajo Nations (Figure 3). The Navajo Nation encompasses an area of 71,000 km^2 extending from northwestern New Mexico to northeastern Arizona and into southeastern Utah. The Hopi Nation (6,557 km^2) is embedded within the Navajo Nation on Black Mesa (Figure 3). Topographic relief is a first-order control on the local climatology including the spatial occurrence, quantity, and seasonal timing of precipitation and groundwater recharge. By extension, it becomes a first-order control on the generation of perennial and ephemeral surface flow on the Navajo and Hopi Nations. Surface flow, in turn, is the primary source of recharge to the alluvial aquifers on the tribal land illustrating the strong interconnections between topography, climatology, geomorphology, and hydrogeology in this region. The most important topographic features in terms of precipitation and recharge are the Chuska Mountains and Black Mesa. Many perennial springs and headwater streams are found in the Chuska Mountains where average annual precipitation can exceed 16 inches. Snowfall and the development of a seasonal snowpack account for most of the precipitation and recharge occurring in the Chuska Mountains. The perennial headwater streams drain into Chinle Wash and during low-discharge conditions, provide recharge to the alluvial aquifer system of Chinle Wash. In comparison, the Black Mesa Basin commonly receives less than 8 inches of precipitation annually and is largely internally drained (Cooley et al., 1969). Snowpack development is thin to non-existent on Black Mesa. Instead, much of the precipitation and nearly all the surface runoff occurs during the North American Monsoon season occurring from June to September (Adams and Comrie, 1997; Aggett et al, 2011). Very little surface runoff from the five, large ephemeral streams draining Black Mesa makes it to the Little Colorado River which is located to the south of tribal land (Figure 3). Yet, these drainages are thought to supply most of the annual sediment load to the Little Colorado River. The runoff not reaching the Little Colorado River represents a

potentially significant amount of alluvial recharge within the ephemeral drainages. However, alluvial recharge processes remain poorly quantified in the Black Mesa washes.

Black Mesa remains the primary source of water for Native Hopi and Navajo communities and water (Macy et al., 2012). The N-aquifer, composed of water-bearing units of Navajo Sandstone and Wingate Sandstone, is the principal deep aquifer of the Black Mesa Basin (Cooley et al., 1969; Macy et al., 2012). In addition, discontinuous deposits of Quaternary alluvium ranging in depths from 30 to 225 feet are present along the wash channels and the alluvial aquifers derived from these deposits represent the primary source of water for springs, hand-dug wells, and water for livestock for communities south of Black Mesa (Cooley et al., 1969). Hydraulic communication between the deeper N-aquifer and the alluvial aquifers has not been thoroughly investigated and also remains poorly quantified (Cooley et al., 1969). Current watershed-scale models of alluvial recharge processes do not account for the discontinuous nature of the alluvial deposits nor their spatial relationship with outcroppings of the N-aquifer. This represents a critical gap in our understanding of groundwater recharge processes in the region since recent data suggest that groundwater levels in the N-aquifer are declining overall (Macy et al., 2012) and there are overall decreases in the quantity and quality of alluvial groundwater south of Black Mesa (Leeper, 2003). Springs along this drainage provide essential sources of water utilized by Native communities for livestock and irrigation of crops (Figure 2). This study aims to improve understanding of groundwater recharge processes in the Oraibi Wash using structural and stratigraphic analysis combined with stable isotope analysis of water. I use δD and δ18O to identify sources of groundwater recharge.

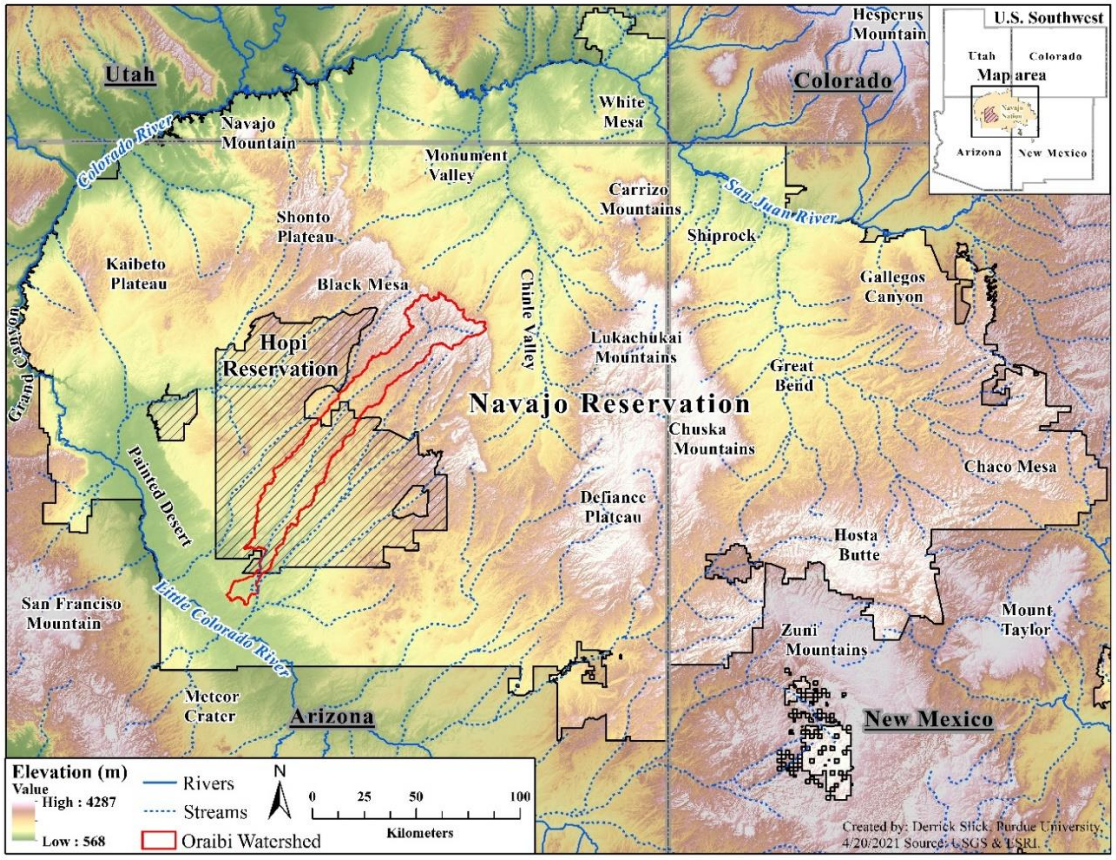

Figure 1– Shaded relief map of the Four Corners region, USA. The Navajo reservation is outlined by a solid black line. The Hopi reservation is marked by a solid black line and the cross-hatched pattern. The focus of this study, Oraibi Wash, is marked by the red line. Note that the headwaters of Oraibi Wash are in Black Mesa and that it drains southwestward into the Little Colorado River.

Figure 2– Open range cattle and horses along Oraibi Wash on the Navajo reservation. Much of the culture of the Navajo Nation is centered on livestock that depend in the open range on springs. This spring is the East Fork Spring along Oraibi Wash.

Chapter Summary

This thesis is divided into three chapters. Chapter 1 outlines the components of the document. Chapter 2 presents new a geologic cross-section of the Oraibi watershed and focuses on the geologic framework and controls on the distributions of springs and groundwater flow at Black Mesa, Arizona. Chapter 3 presents stable water isotope measurements of δD (Deuterium/ hydrogen) and δ18O (Oxygen-18) from precipitation, springs, and wells between June 2018 to December 2019. These data are then used to delineate the sources of groundwater recharge in the Oraibi watershed.

Chapter 2 presents a geologic cross-section across the north side of Black Mesa. The cross section defines a series of monoclines, anticlines, and synclines that control the distribution of springs in Oraibi Wash. The cross section also demonstrates the stratigraphic controls on the distribution of springs in the area. The stratigraphy and structures of Black Mesa are a product of

the Mesozoic Sevier and Laramide orogens of the western Cordillera. At a regional scale, the springs of Black Mesa are related to the interactions between these geologic features and where they intersect with the cliffs, canyons, and mesas of northeastern Arizona. Springs on the Black Mesa are intimately connected by the geology and the landscape.

Chapter 3 consist of utilizing a data set based on 49 samples from precipitation collectors and 77 groundwater (43 springs & 34 wells) samples to provide an understanding groundwater recharge. The isotope ($\delta^{18}O$) tracer concentration allowed us to calculate the fraction contribution of winter versus monsoon precipitation to the groundwater of Black Mesa. With data from one and half water year, we were able to identify seasonal variations in stable isotopes (winter vs. monsoon) and delineate seasonal variability in groundwater recharge along Oraibi Wash.

CHAPTER 2. GEOLOGIC FRAMEWORK OF BLACK MESA, ARIZONA: STRATIGRAPHIC AND STRUCTURAL CONTROLS ON SPRING DISTRIBUTION IN ORAIBI WASH

Introduction

This chapter delineates the stratigraphic and structural controls on the distribution of springs used by Navajo and Hopi communities along Oraibi Wash. Our analysis began field identification of the stratigraphic position of springs along Oraibi Wash, next, field collection and compilation of previously published structural data, mainly bedding attitudes were completed, in formations along the wash. Third, construction of a regional cross section to illustrate the geologic location and structural controls on spring distribution using ARCGIS and Adobe Illustrator (Figure 3). Major springs studied in our analysis are from northeast to southwest including Spruce Springs, Shonto Spring, Prairie Dog Spring, Oraibi Spring, Ash Well, and Hat Spring. The locations of these springs are shown in Figure 3C.

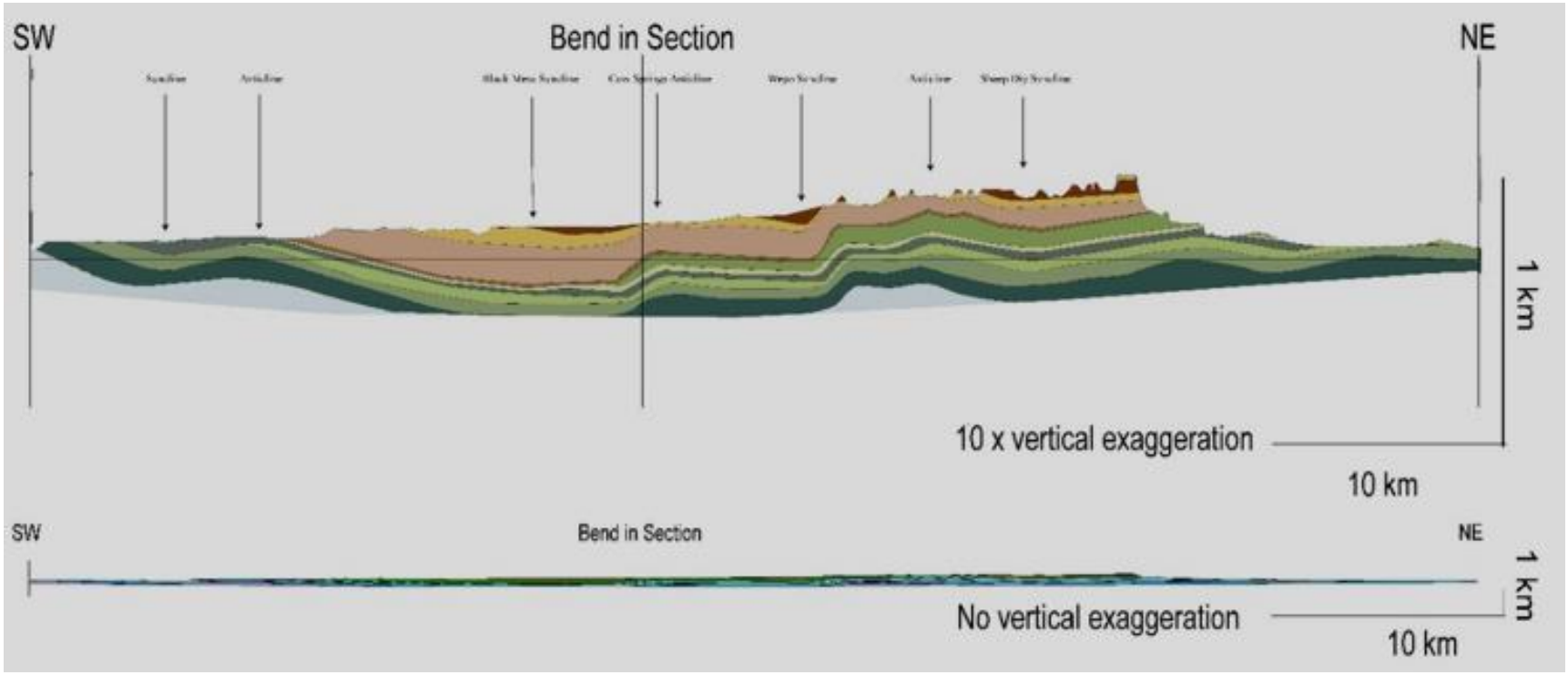

Figure 3. A) Structural cross section through Black Mesa that trends northeast-southwest. See Figure 4 for location of cross section. Note that there are a series of broad anticlines and synclines that are discussed in the text.

Figure 3 continued

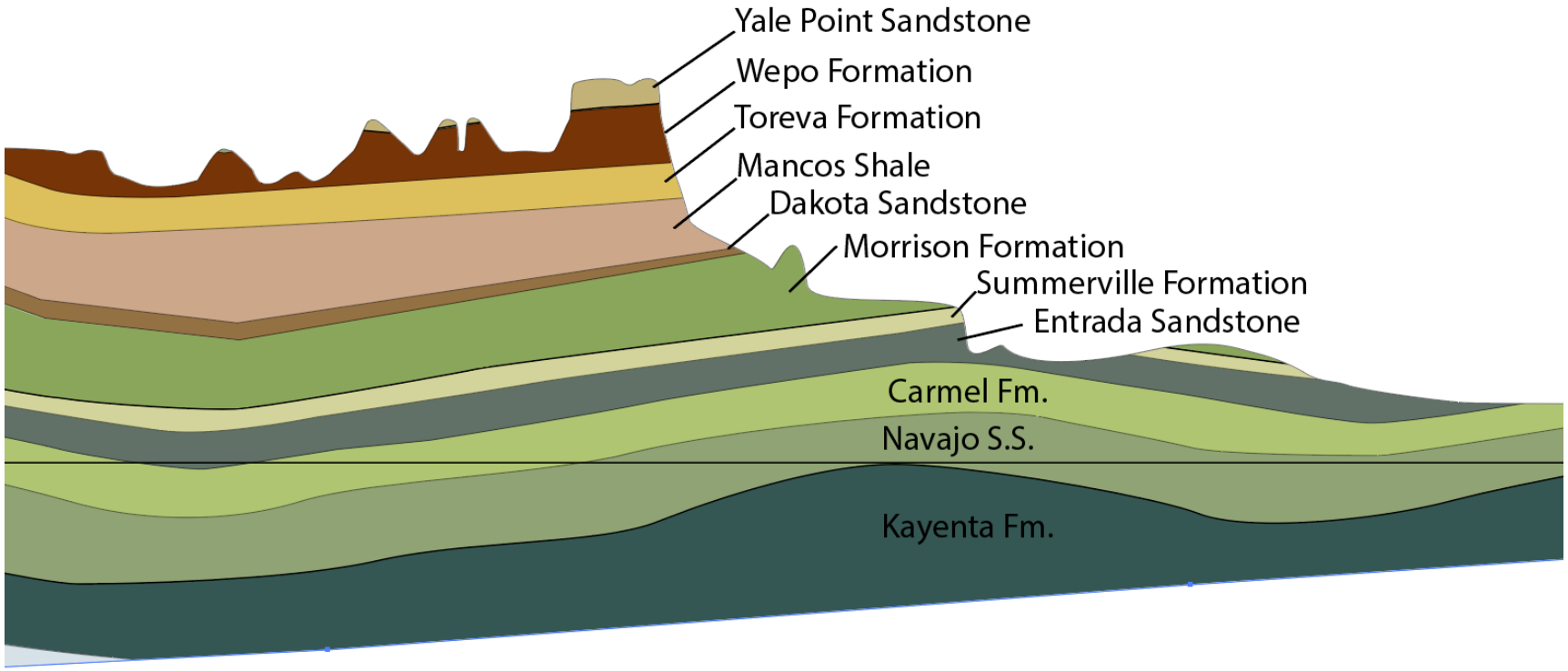

B) Same structural cross-section with no vertical exaggeration.

Figure 3 continued

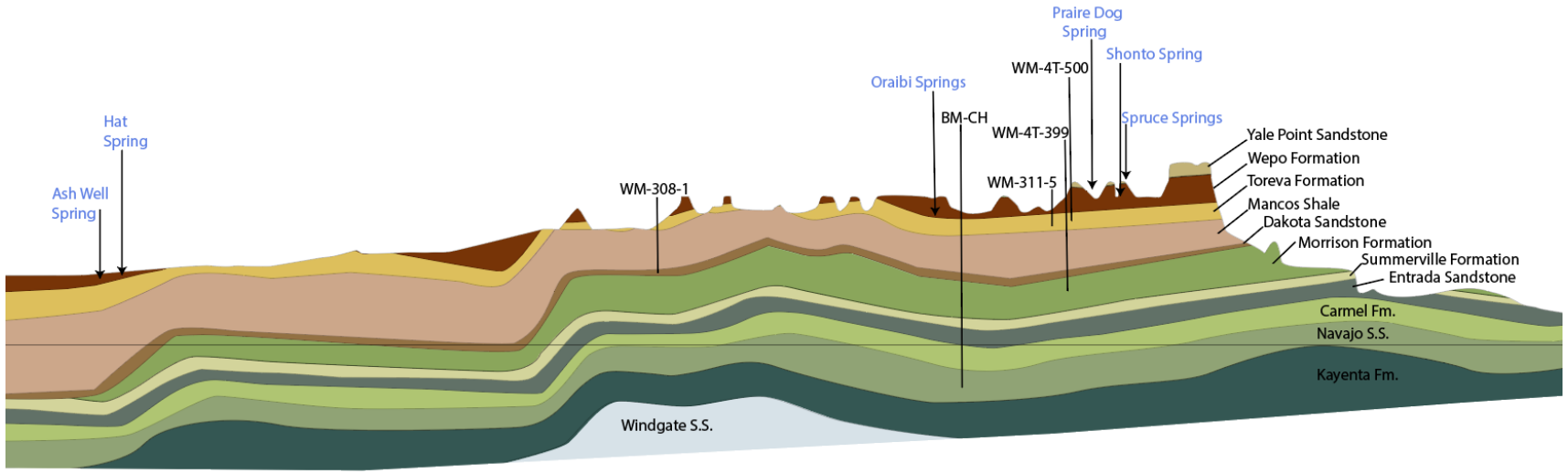

C) Enlargement of cross-section shown in Figure 3A with the springs labeled that are the focus of this study.

We also visited several more minor, ephemeral springs that are not shown in Figure 3C. To our knowledge, Figure 3C is the first cross section constructed through Black Mesa showing the location of springs as they relate to the underlying geologic framework. We interpret the results of this part of the study to show that there are two different types of springs along Oraibi Wash. The first type, what we term as stratigraphically controlled springs, emerge from horizontal bedding layers where more permeable strata are adjacent to impermeable strata. These types of springs are best exposed in the upper part of Oraibi Wash. Here the youngest formations, the Wepo Formation, and the Yale Point Sandstone, crop out along Oraibi Wash. A second type of spring that we term as structurally controlled springs emerge from fracture systems in thicker sandstone beds. These types of springs are best exposed in the Toreva Formation in the middle part of Oraibi Wash. Deformation of this thick sandstone unit results in vertical fractures that are concentrated along anticlines and monoclines that have deformed the Upper Cretaceous strata exposed in Oraibi Wash.

Geologic Background and Previous Studies: Stratigraphy and Structures of Black Mesa

Black Mesa is part of the Cordilleran foreland basin system that extends from Mexico to Alaska (Dickinson, 2009). Strata of the Mesozoic foreland basin are important sources of groundwater, coal, and hydrocarbon resources for much of North America. Stratigraphically, at Black Mesa, the Mesozoic strata are represented from the Jurassic Entrada Formation to the Upper Cretaceous Yale Point Formation (Figure 3). All these strata are well exposed along the eastern escarpment of Black Mesa (Figure 2B). Coal beds in the Wepo Formation (Figure 2C) have historically been mined by the Peabody Coal Company for electricity generation. In this section we outline the stratigraphy of Black Mesa in our study area. For more details on the local stratigraphy see Eaten et al. (1987) and Franczyk, (1988), and for more regional stratigraphic and tectonic context of the Mesozoic foreland basin see DeCelles (2004).

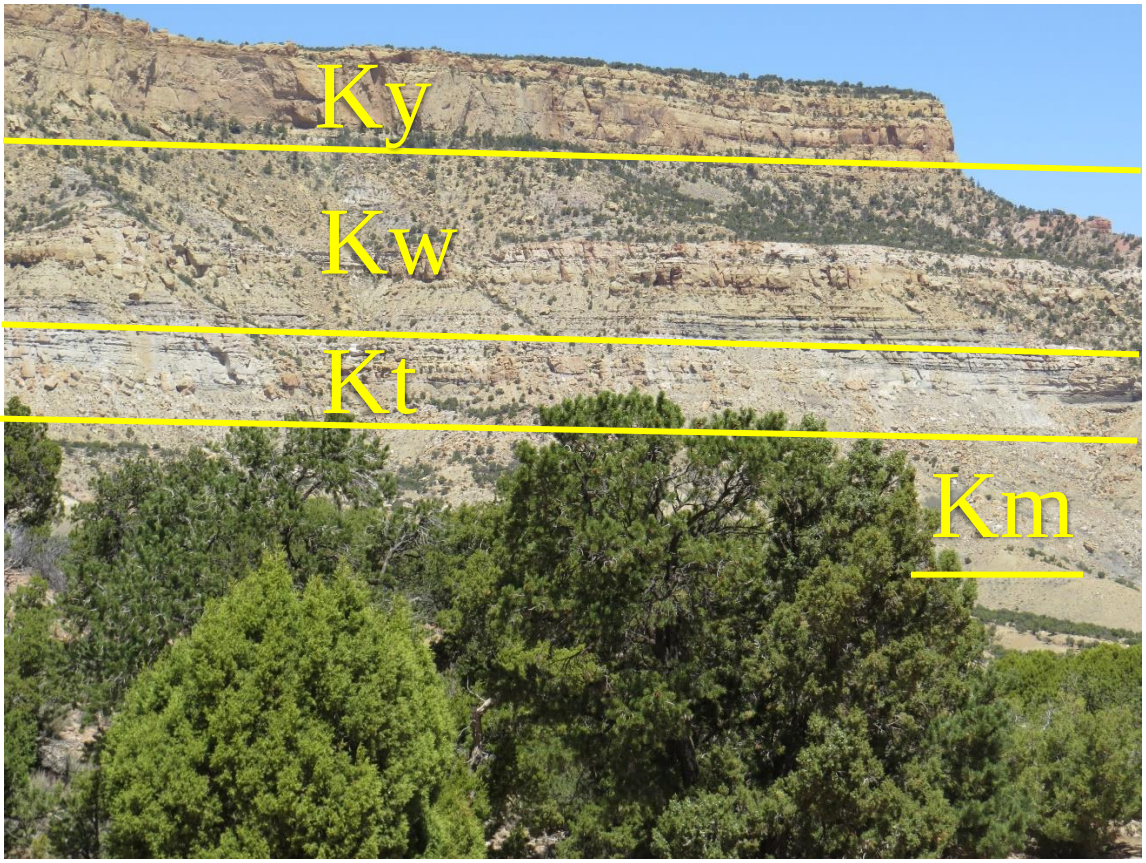

Figure 4 - The eastern escarpment of Black Mesa with the stratigraphy grouped and labelled. Ky, Yale Point Sandstone; Kw, Wepo Formation; Kt, Toreva Formation; Km, Mancos Shale; the Dakota Formation is out of view below the bottom of photo.

The Upper Cretaceous stratigraphic formation exposed along Oraibi Wash that are important for our analysis are the Dakota Sandstone, Mancos, and Mesa Verde Group. An important aquifer for the Navajo Tribe is the D-aquifer which is hosted in the Dakota Sandstone has been divided by (Haven, 1991) into three members: an upper sandstone that has lenticular geometries that range in thickness from 15 – 35m, a finer-grained middle member that is characterized interbedded shale, siltstone, sandstone, and coal, and a lower sandstone member with low-angle planar and trough cross stratification. The Dakota Sandstone has 23-28% porosity and coefficient of permeability range from 0.7 – 25gpd per sq. ft. (Cooley et al., 1969). The Mancos Shale overlies the Dakota Sandstone in the Black Mesa area (Figure 3). The Mancos Shale inter-tongues with the Upper Dakota Sandstone and Lower sandstone of the Toreva Formation. Four members have been defined for the Mancos Shale: a lower fossiliferous calcareous shale member, a middle well laminated calcareous shale member, the Hopi sandy member, and the upper non calcareous claystone member (Haven, 1995).

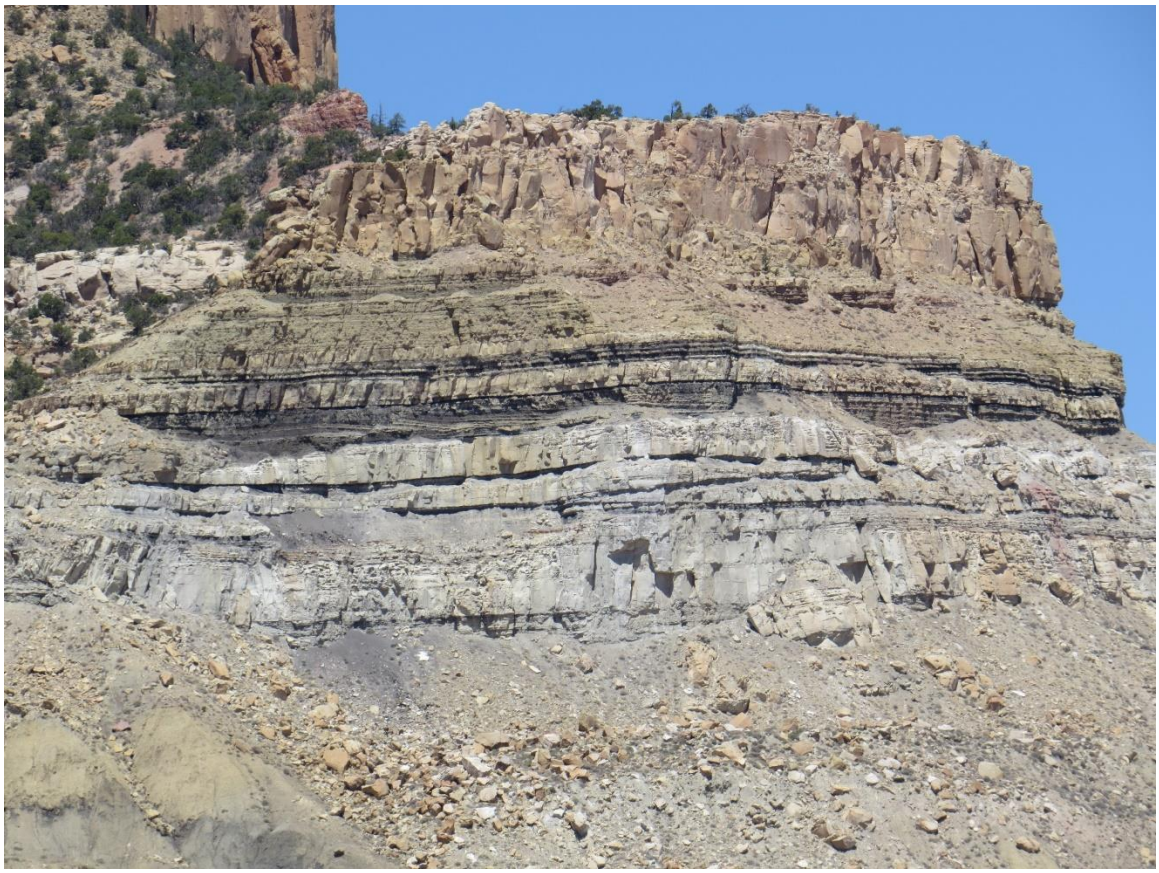

Figure 5- Close-up photograph of the coal seams in the Wepo Formation that have been the focus of coal mining for several decades on Black Mesa.

The Toreva Formation overlies the Mancos Shale (Figure 3). This formation consists of fine to coarse sandstone with interbedded siltstone and carbonaceous shale. The Toreva Formation has a porosity between 29 – 34 percent and coefficients of permeability ranges from 0 – 534 gpd per sq. ft. (Cooley et al., 1969). This formation is well exposed in higher elevations along the middle and upper reaches of the Oraibi Wash. The Upper Cretaceous Wepo Formation is characterized by siltstone interbedded with sandstone and coal. It has a previously reported porosity between 1 – 2 percent and coefficients of permeability from 0.0009 – 0.02 gpd per sq. ft. (Coolie et al., 1969). Coal seams in the Wepo Formation have low sulfur and ash with BTU's above 12,000, and are commercially mined (Haven, 1995). Coal of the Cretaceous Wepo Formation was mined by Peabody Energy from the 1970's until November 2019. In northeastern Black Mesa, The Yale Point Sandstone is stratigraphically the highest formation. This formation is exposed in the higher topography of Black Mesa. Cooley et al., did not report the porosity or calculate the coefficient of permeability for the Yale Point Sandstone (1969).

Structurally, the strata of Black Mesa have a regional dip of 4 to 5 degrees to the southwest as shown on Figure 3. The modern rivers that drain Black Mesa, like Oraibi Wash, Moenkopi Wash, Dinnebito Wash, Wepo Wash, Polaccu Wash are tributaries of the Little Colorado River (Figure 1). Superimposed on the regional dip are a series of broad, shallow-dipping syncline, anticline, and monoclinal structures (Figures 3, 4). Along the eastern part of Black Mesa these structures include Sheep Dip Syncline, Tochee Monocline, Oraibi Monocline, and Wepo Syncline. Along the western part of Black Mesa, these structures include Cow Springs Anticline, Black Mesa Anticline, Mount Beautiful Anticline, and Howell Mesa Anticline. These structures were originally recognized by the geologic mapping of Cooley et al. (1969).

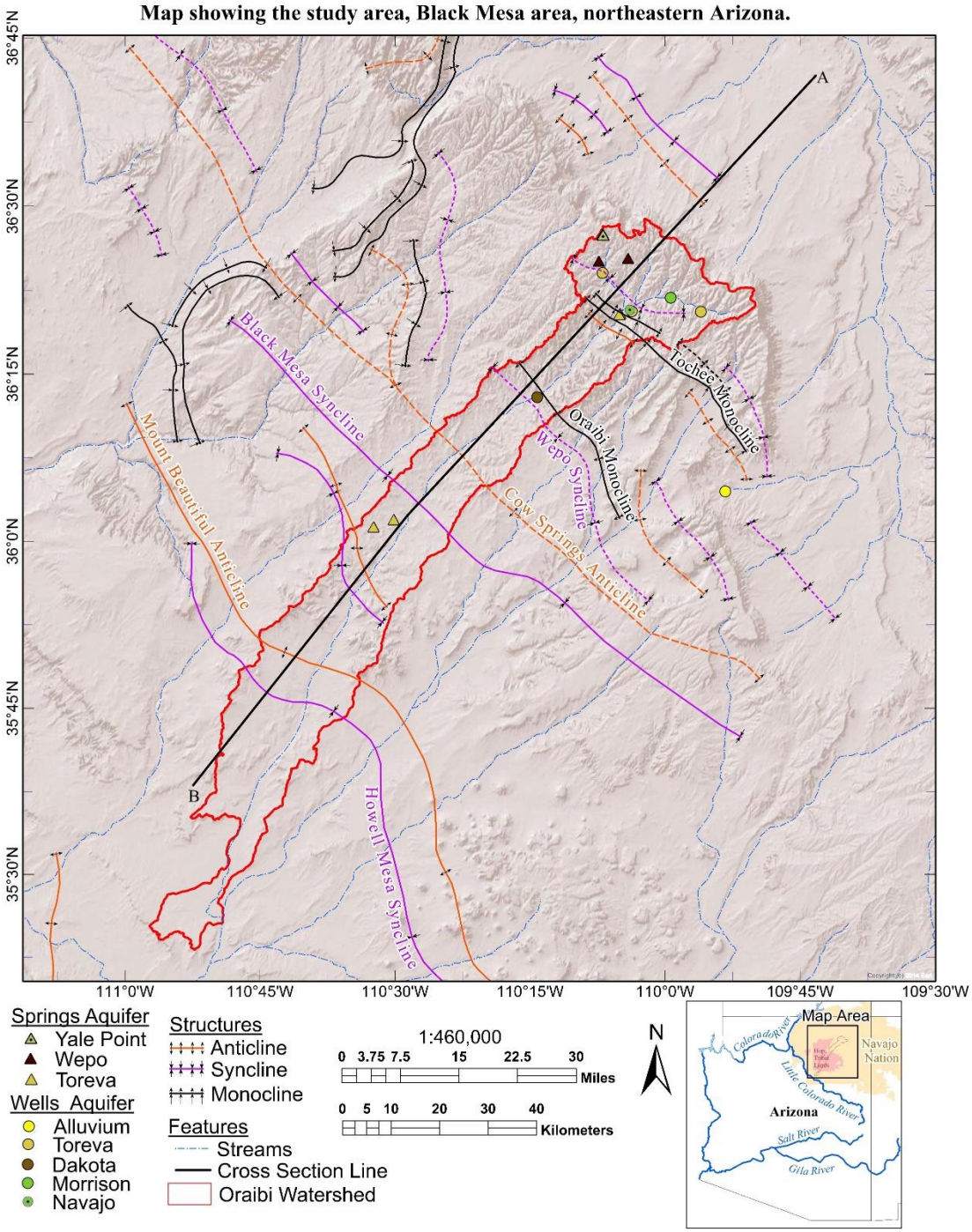

Figure 6– Map showing line of cross section shown in Figure 3, the locations of major anticlines and synclines, and springs along Oraibi Wash that the focus of this study.

Materials and Methods

The Oraibi Watershed encompasses about 1,896 square kilometers within the LCR basin. Regional geologic structures in northern Arizona were based on published U.S Geological Survey (USGS) report from Cooley et al. (1969). At the request of Bureau of Indian Affairs (BIA) and Navajo Tribe, the USGS took inventory of springs and wells, investigated the geology and groundwater resources, and developed groundwater supply for livestock, institutions, and industrial operations throughout the Navajo Nation (Cooley et al., 1969, p.A2).

Geologic maps from the Cooley et al. (1969) report was download from the USGS website in 2017. Maps were geo-referenced using the ARCGIS software, acquired data include synclinal, anticlinal, and monoclinal structures, dips, and orientations from the limbs of folds. Strike and dips collection are from a 20 km swath centered along the cross-section line. The degree of dips was then multiplied by 10 for exaggerated effects, this was necessary for the geologic framework.

Geology units used in the cross-section were compiled from several authors: USGS with U.S. Atomic Energy Commission; O'Sullivan and Beikman (1963) Shiprock quadrangle, USGS with U.S. Energy Research and Development Administration; Haynes and Hackman (1978) Marble Canyon quadrangle, USGS in cooperation with U.S. Energy Research and Development Administration; Hackman and Olson (1977) Gallup quadrangle, and USGS in cooperation with U.S. Department of Energy; Ulrich et al. (1984) Flagstaff quadrangle.

Complied maps of 1° X 2° quadrangle geologic maps were download from the USGS website in 2017. Individual maps were geo-referenced using ARCGIS software, gathered data include structures, measured intervals of geologic units, and lithology descriptions.

The Navajo Nation Water Management Branch (2017) and Navajo Tribal Utility Authority (2018) in Fort Defiance, AZ provided well log information from windmills and public water system drilling logs. Well log information was used to across reference the thickness of sedimentary layers from within the Oraibi Watershed. Well logs are from the following wells: Kitsillie Well #1 (04T-521), Hardrock Well #2 (04-0580), War Path Valley (4T-399), and Wind Rock Valley (4T-500). Longitude and latitude coordinates from well logs were used to reference their locations. Thickness of geologic units were then compared to Cooley et al. (1969) stratigraphy, well depths and clay screens were verified and placed in the estimated sedimentary layer.

The field work included the measurement and descriptions of lithology near spring sampling sites. Geologic units from the quadrangle maps, mentioned above were verified in the field with lithology from Cooley et al. (1969) and Haven (1995).

Results

Our field analysis identified two primary types of springs within the Oraibi Wash. Stratigraphically controlled springs are the product of the juxtaposition of permeable sandstone against low-permeability mudstone. These types of springs are also associated with coal beds that are common in Upper Cretaceous formations along Black Mesa. Major stratigraphically controlled springs include Spruce Springs, Shonto Spring and Prairie Dog Spring shown in Figure 3. Figure 5A is of Shonto Spring and shows a spring emerging from the Wepo Formation. The porosity and permeability contrasts between the underlying gray siltstone and the overlying sandstone produce a horizontal flow path for groundwater. The sandstone is the ledge former in the gully in the photo. The person with the grey shirt is standing on the sandstone bed whereas the person in the foreground is standing on the underlying siltstone. Figures 5B-C show a spring emerging from a coal bed in the Toreva Formation. These types of springs are often stained orange red in color indicative of high iron content in springs emerging from coal beds of Black Mesa.

Figure 7– Photograph of Shonto Springs that emerges from the Wepo Formation. This is an example of what we classify as a stratigraphically controlled spring in this study. See text for additional discussion.

A second type of spring documented in Oraibi Wash are termed structurally controlled springs. These springs emerge from vertical fractures in the Toreva Formation that intersect Oraibi Wash. Examples of these types of springs are Oraibi Springs, Ash Well, and Hat Spring shown in Figure 3. Figure 6 show photographs from Oraibi Spring providing an example of a structurally controlled spring. These types of springs are common in the Toreva Formation where it has been fractured on the limbs of the Tochee Monocline and the Cow Spring anticline (Figure 3C). Note in Figure 5 the pervasive vertical fracture pattern in the Toreva Formation. This fracture pattern results in multiple springs at one location and larger discharges in the structurally controlled springs. West Fork Spring as shown in Figure 6 E, F, is another example of a structurally controlled spring within thick sandstone of the Toreva Formation. This spring is a minor spring and is not shown on Figure 3.

Figure 8- Stratigraphically-controlled spring emerging from a coal bed in the Toreva Formation. Springs along Oraibi Wash associated with coal beds often have a stained orange-red color.

Figure 9- A – Photographs of structurally-controlled springs that are common along the limbs of anticlines exposed along Oraibi Wash. Note spaced vertical fractures at Oraibi Springs and location of spring at the fracture in the center of the photograph.

Figure 9 continued

B (top) and 6 - C (bottom) Close-up photograph of the multiple springs emerging from fractures in bedrock at Oraibi Springs.

Figure 9 continued

D) Overview photograph of the multiple springs emerging from fractures in bedrock Oraibi Wash. Note cow in center of photograph for scale.

From a wider regional perspective, our analysis documents the type of springs within Oraibi Wash change downstream. However, upstream, (a) exists stratigraphically controlled springs are more common. The Wepo Formation and Yale Point Sandstone crop out along the upper parts of Oraibi Wash. In these formations the lithology decreases or increase in porosity and permeability that focus groundwater flow to specific units. The stratigraphically controlled springs are best developed where permeable strata are adjacent to impermeable strata resulting in horizontal flow paths that are the sources of groundwater for these types of springs. The abundant, highly fractured, coal beds in the Wepo Formation also form horizontal conduits for groundwater that create springs when those beds crop out in Oraibi Wash. In contrast, in the middle part of Oraibi Wash, the springs more commonly are sourced by groundwater flowing out of vertical fractures. The Toreva Formation is the formation that most commonly crops out along this part of Oraibi Wash. The Toreva Formation is a thick-bedded sandstone (Figure 6C) that is more highly fractured along the broad anticlines and synclines that are will exposed in Oraibi Wash (Figure 3C). These structurally-controlled springs are often characterized by multiple nearby springs each emanating from a fracture, and often result in ponded water throughout the summer that is used extensively by the Navajo communities and their livestock.

Figure 10 - A (top) and B (bottom) West Fork Springs is another example of a structurally controlled spring located on a fracture in the Toreva Formation.

References

Adams, D.K. and Comrie, A.C. (1997) The North American Monsoon. Bulletin of the American Meteorological Society, 78, 2197-2213. http://dx.doi.org/10.1175/1520-0477(1997)078<2197:TNAM>2.0.CO;2

Aggett, G., M. Frisbee, B. Harding, G. Miller, and P. Weil. 2011. Hydromet Network Optimization for the Navajo Nation's Department of Water Resources Water Management Branch, AMEC Consulting Report

Cook, E. R., Woodhouse, C. A., Eakin, C. M., Meko, D. M., & Stahle, D. W. (2004). Long-term aridity changes in the western United States. *Science*, 306, 1015- 1018. https;//doi.org/10.1126/science.1102586

Cooley, M.E., and Harshbarger, J.W., Akers, J.P., and Hardt, W.F., 1969, Regional Hydrogeology of the Navajo and Hopi Indian Reservation, Arizona, New Mexico, and Utah: U.S. Geological Survey Professional Paper 521-A.

DeCelles, P.G., 2004, Late Jurassic to Eocene evolution of the Cordilleran thrust belt and foreland basin system, western USA: American Journal of Science, v. 304, p. 105-168, doi: 10.2475/ajs.304.2.105.

Dickinson, W.R., 2009, Anatomy and global context of the North American Cordillera, in Kay, S.M., Ramos, V.A., and Dickinson, W.R., eds., Backbone of the Americas: Shallow subduction, plateau uplift, and ridge and terrane collision: Geological Society of America Memoir, 204, p. 1-29.

Eaton, Jeffrey G., and J. Dale Nations. "Introduction; Tectonic Setting Along the Margin of the Cretaceous Western Interior Seaway, Southwestern Utah and Northern Arizona." *Special Paper - Geological Society of America* 260 (1991): 1–8. Web.

Franczyk, K.J. "Stratigraphic Revision and Depositional Environments of the Upper Cretaceous Toreva Formation in the Northern Black Mesa Area, Navajo and Apache Counties, Arizona." *US Geological Survey Bulletin* 1685 (1988): n. pag. Print.

Hackman, R.J., Olson, A.B., 1977, Geology, Structure, and Uranium Deposits of the Gallup 1º x 2º Quadrangle, New Mexico, and Arizona, Miscellaneous Investigations Series Map I-981 (Sheet 1 of 2).

Haven, H.W., Jr., 1997, Stratigraphy and Coal Resources of the Wepo Formation (Late Cretaceous), Black Mesa Basin, Northeastern Arizona: Thesis Submitted for Master of Science in Geology, Northern Arizona University.

Haynes, D.D., and Hackman, R.J., 1978, Geology, Structure, and Uranium Deposits of the Marble Canyon 1º x 2º Quadrangle, Arizona, Miscellaneous Investigations Series Map I-1003 (Sheet 1 of 2).

Leeper, J.W., 2003, Navajo Plans for their water future. New Mexico water planning 2003, New Mexico Water Resources Research Institute. https://nmwrri.nmsu.edu/wp-content/uploads/2015/watcon/proc48/leeper.pdf

Macy, P., Brown, C.R., Anderson, J.R., 2012, Groundwater, surface-water, and water-chemistry data, Black Mesa Area, northeastern Arizona – 2010-2011, Open-File Report 2012-1102, United States Geological Survey, Reston, VA.

Milly, P. C. D., & Dunne, K. A. (2020). Colorado River flow dwindles as warming-driven loss of reflective snow energizes evaporation. *Science*, 367, 1252-1255. http://doi.org/10.1126/science.ayy9187

O'Sullivan, R.B., and Beikman, H.M., 1963, Geology, Structure, and Uranium Deposits of the Shiprock Quadrangle, New Mexico, and Arizona, Miscellaneous Geologic Investigations Map I-345 (Sheet 1- Geology).

Overpeck, J., & Udall, B. (2010). Dry times ahead. Science, 328, 1642–1643. http://doi.org/10.1126/science.1186591

Ulrich, G.E., Billingsley, G.H., Hereford, R., Wolfe, E.W., Nealey, L.D., and Sutton, R.L., 1984, Map Showing Geology, Structure, and Uranium Deposits of the Flagstaff 1º x 2º Quadrangle, Arizona, Miscellaneous Investigations Series Map I-1446 (Sheet 1 of 2).

CHAPTER 3. SEASONALITY OF RECHARGE

Introduction

Statement of the Problem:

The southwestern United States is land of rugged topography shaped by a semiarid climate. Even small amounts of changes in precipitation in this landscape can have dire impacts on human communities, animals, and plant ecosystems. This area is currently and has historically been very vulnerable to droughts. (Cook et al., 2004, Milly & Dunne, 2020; Overpeck & Udall, 2010). Currently there is widespread concern, for example, on the extremely low flows in the Colorado River and the low volumes of water in Lake Powell and Lake Mead due to a prolonged drought. The Colorado River and the reservoirs located along the river provide drinking water, agricultural irrigation, and electricity to many communities in the region. This watershed is the lifeblood of much of the southwestern U.S.

Indigenous communities located along this watershed are in a particularly dangerous situation because of their rural land base, traditional agricultural lifestyle, and minimal infrastructure. The Navajo Nation's environmental vulnerability is exacerbated by added stress to water resources due to additional factors that include poverty, poor land and water management, and ineffective water governance. As a vulnerable region, the Navajo Nation must take critical steps to prevent disastrous events for its people and economy and to reduce the strain on limited water sources. One step the Navajo Nation can take is to plan for the increased warming, drought, and water deficiencies by generating the knowledge themselves to help assist in planning, management, and mitigation. The goal of this study is to evaluate the sources of groundwater recharge along a major wash that provides water to Navajo and Hopi communities in northeastern Arizona. While a few studies have analyzed the more regional aspects of water resources on the Navajo reservation, few studies have done a detailed analysis of a local watershed. This study focuses on sources of groundwater recharge along Oraibi Wash. This drainage is in Black Mesa, Arizona in the heart of the Navajo and Hopi reservations and is a tributary of the Little Colorado River (Figure 3.1). The hypothesis I plan to test with this study is that the higher elevations along the Oraibi Wash accumulate more snowpack melt that contributes more to groundwater recharge than the monsoon influence at lower elevations.

Sources of Precipitation on the Navajo Nation

There are two sources of precipitation in this region: summer monsoon and winter snowpack. Winter precipitation provides 30% to the annual precipitation in the U.S. Southwest (Jana et al., 2018). Tulley-Cordova et al. (2018) collected four years of precipitation data from the Navajo Nation to study the drivers of the North American summer monsoon. The summer monsoon is mostly driven by convective storms and tropical cyclones. The winter snowpack, in contrast, is mainly driven by midlatitude cyclonic systems (Jana et al., 2018). These previous studies documented that (1) Summer monsoon consistently provided heavy daily rainfall rates that were less variable than pre- and post-monsoon season rainfall values; (2) Rainfall amounts increased slightly with increasing elevation and precipitation; and (3) Moisture recycling through land surface evaporation and transpiration were shown to increase monsoon precipitation in the region. Precipitation from the summer monsoon can be characterized as extremely violent and short-lived storms (Earman et al, 2006.). In a matter of minutes, massive amounts of rain runoff fill dry channel beds. However, it remains unclear what role snowmelt plays in compared to monsoon runoff to groundwater recharge processes.

Compared to its monsoon counterpart, winter snowmelt occurs over a much longer period when evapotranspiration rates are low. Thus, snowmelt runoff can infiltrate the soil, percolate through the rooting zone, and a greater proportion often makes it to the aquifer to become recharge. Thus, snowpack melt, therefore, seems like it may be more important to recharge than monsoon runoff for groundwater recharge but this inference has not been tested along Oraibi Wash. Previous studies have estimated that snowmelt provides at least 40 – 70% of groundwater recharge in high elevations in the southwestern U.S. (Earman et al, 2006). Data collected by the Navajo Nation Department of Water Resources showed that between 1985-2014 there was no trend in increasing or decreasing in snowpack for the Chuska Mountains and Defiance Plateau (Tsinnajinnie et al, 2018). Springs in the headwaters depend on winter precipitation for groundwater recharge and is the primary source of water for local human communities, livestock, and wildlife.

Monsoon rainfall and snow accumulation vary by elevation. Higher elevations tend to have greater precipitation amounts due to higher snowfall. In comparison, the monsoon rains are more sporadic in temporal-spatial distribution and less controlled by elevation.

Stable Isotope Hydrology

Environmental isotopes in hydrology are naturally occurring elements used to trace groundwater provenance to understand the recharge processes and subsurface flow paths (Clark and Fritz, 1997). Conservative tracers' oxygen ($^{18}O/^{16}O$) and hydrogen ($^{2}H/^{1}H$) stable isotope ratios in precipitation are temperature dependent; therefore, there is a seasonal variability. Summer precipitation is enriched in the heavier isotopes, while winter precipitation is less enriched. These seasonal differences can be used to partition groundwater into summer and winter recharge components (e.g., Simpson et al., 1970 & Winograd et al., 1998). Although there are some complications that must be considered. For example, rain and snow can change isotopically through evaporation before infiltrating into the subsurface ground (e.g., Earman et al., 2006, Clark & Fritz, 1997). Using statistically distinct seasonal endmembers from winter precipitation and summer surface-water run-off, a mixing model can be created using $\delta^{18}O$ or δD to estimate the faction recharge from winter precipitation (e.g., Solder & Beisner, 2019, Eastoe and Wright, 2019, Zamora et al., 2020, Ginzalez-Trinudad et al., 2017).

To test my hypothesis that winter precipitation/winter snowmelt has greater influence and is the primary source of groundwater recharge for the Oraibi watershed, I utilized the stable isotope partitioning method. For one and a half years, samples were collected from 9 springs and 7 wells. A total of 10 collection stations were used to collect a total of 49 samples of winter and summer precipitation along Oraibi Wash. These samples were analyzed in the Stable Isotope Ecology and Hydrology Lab at Purdue University under the supervisor of Dr. Lisa Welp. Then using the two end members of winter and summer precipitation, I calculated the fraction of winter precipitation that contributes to groundwater recharge in Oraibi Watershed of the Navajo Nation in Arizona.

Methods

Sampling methods

Water samples were collected from 6 sampling events, roughly every quarter of the year starting from June 2018 to October 2019. Collected samples were filled in plastic Falcon tubes stored in zip-lock bags inside a food-free icebox with dry ice (-80°C) and shipped overnight via FedEx from Flagstaff, AZ to Purdue University.

Precipitation was collected using a 1-L Nalgene container connected to a 7.7 cm (3 in.) stainless steel funnel with a 6.35 mm (.25 in.) diameter polyvinyl chloride (PVC) hose. Collectors were housed inside a 7.7 cm (3 in.) diameter PVC pipe that had a total length of 61 cm (24 in.) with 30.5 cm (12 in.) buried in the ground. Nalgene containers were pre-filled with mineral oil ranging from 20 – 25 grams to reduce evaporation from containers. A total of 10 collectors were placed within the Oraibi watershed in areas with road access. Collected precipitation waters were weighed in the field using a digital scale then sealed with electrical tape around the caps and placed in an icebox with 2 kg (4.5 pounds) of dry ice. Groundwater samples were collected from the springs (mainly seeps), and wells were sampled from water holding tanks that are fed by pumping groundwater. Water was sampled from tanks outlet valves after allowing 3 minutes of flow in a 50-mL wide-mouth sample bottle. Sample bottles were sealed with electric tape then placed in an icebox with 2 kg (4.5 pounds) of dry ice.

Earthen dam water samples (if available at the time of sampling) were collected in a 50-mL wide-mouth sample bottle, 5 m (16.40 ft.) from the littoral zone using a 6 m (20 ft.) pole, approximately 15.24 cm (6 in.) below the water surface. Sample bottles were sealed using electrical tape then placed in an icebox with 2 kg (4.5 pounds) of dry ice. These samples were analyzed but are not discussed in this chapter. All data from these samples are presented in the Appendix.

Sampling locations

The Oraibi watershed spans across an area of 1,896 square kilometers of open country that can be extremely difficult during the monsoon seasons. Precipitation collectors were placed in areas with road accessibly. A total of ten precipitation collectors (table 3.1), nine springs (table 3.2), seven wells (table 3.3), were collected and analyzed for this project (Fig. 3.1).

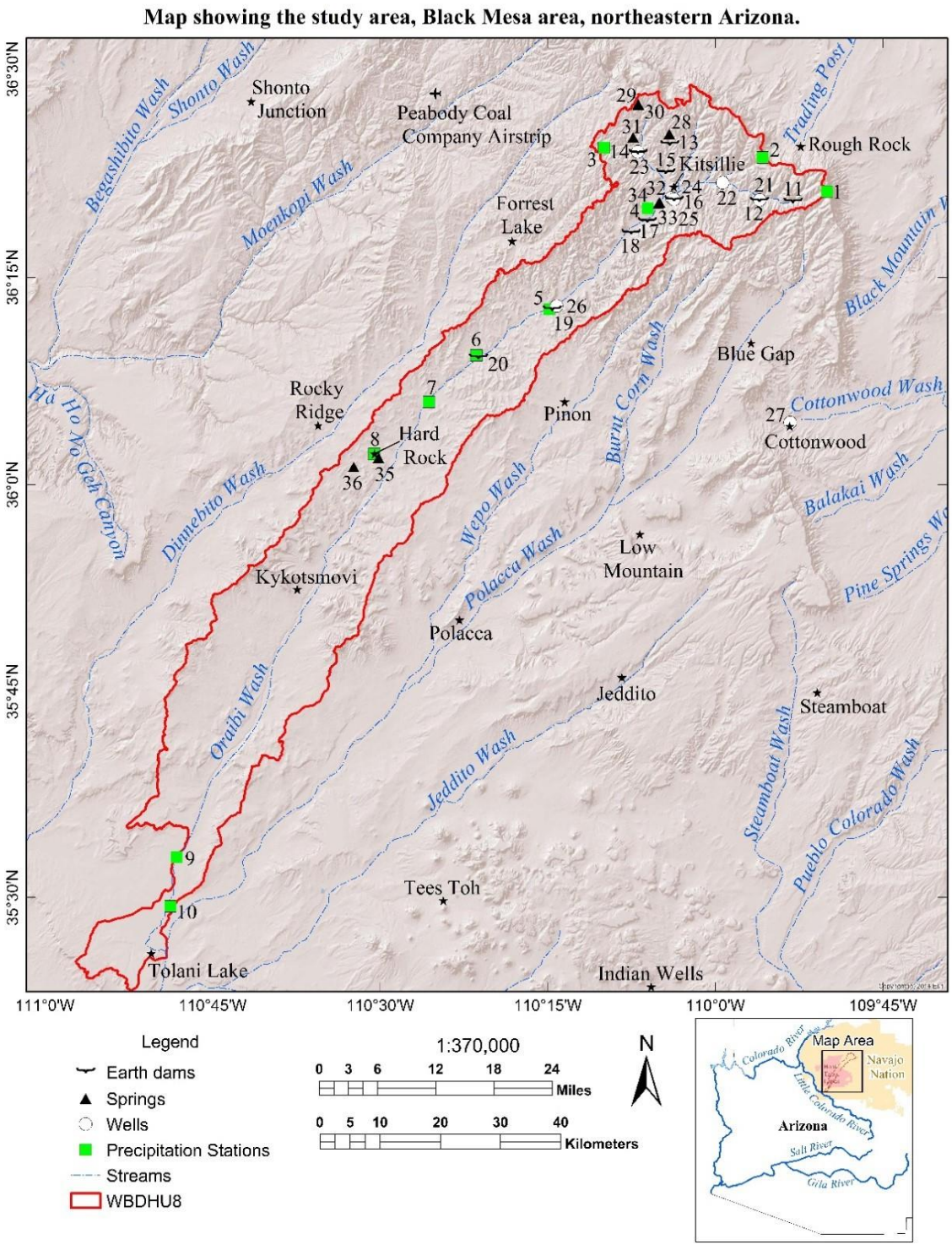

Figure 11 - A map showing the sampling area with site numbers.

Table 1 - Precipitation collectors.

Site #	Site ID	Location name	Lat.	Long.	Elevation (ft.)
1	WRV-P01	Wind Rock Valley	36.35310	-109.83360	8010
2	WPV-P01	War Path Valley	36.39375	-109.92972	7312
3	BRW-P01	Black Rock Wash	36.40569	-110.16610	7378
4	HRV-P01	Hole in the Rock Valley	36.33285	-110.10101	7093
5	IR-41-P01	Indian Route 41	36.21147	-110.24763	6282
6	JUA-P01	Joint Use Area #1	36.15595	-110.35641	6187
7	JUA-P02	Joint Use Area #1	36.09967	-110.42729	5965
8	HRC-P01	Hard Rock Chapter	36.03690	-110.50870	6033
9	TL-P01	Tolani Lake #1	35.54913	-110.80348	4957
10	TL-P02	Tolani Lake #2	35.48941	-110.81277	4888

Table 2 - Springs sampled in Oraibi Wash.

Site #	Site ID	Location name	Lat.	Long.	Elevation (ft.)	Formation
28	SPR-SSA	Sunshine Spring	36.42215	-110.06879	7076	Wepo
29	SPR-SS2	Spruce Spring #2	36.45716	-110.11485	7192	Yale Point
30	SPR-SS1	Spruce Spring #1	36.45813	-110.11546	7198	Yale Point
31	SPR-PD	Prairie Dog Spring	36.41806	-110.12286	7063	Wepo
32	SPR-OS1	Oraibi Spring #1	36.33984	-110.08345	6559	Toreva
33	SPR-OS2	Oraibi Spring #2	36.33987	-110.08316	6559	Toreva
34	SPR-OS3	Oraibi Spring #3	36.33836	-110.08494	6559	Toreva
35	SPR-HS	Hat Springs	36.03241	-110.50233	5999	Toreva
36	SPR-AWS	Ash Well Springs	36.02149	-110.53964	5970	Toreva

Table 3 - Wells Sampled in the Black Mesa area.

Site #	Site ID	Location name	Lat.	Long.	Elevation (ft.)	Formation
21	WM-4T-500	Wind Rock Valley	36.342897	-109.933862	7021	Toreva
22	WM-4T-399	War Path Valley	36.3637	-109.98949	6814	Toreva
23	WM311-5	Black Rock Wash	36.400676	-110.115992	6844	Mancos
24	WM311-4	Kitsillie	36.3437	-110.0617	6694	Toreva
25	BM-CH	Black Mesa Chapter House	36.345659	-110.065268	6703	Navajo
26	WM-308-1	Oraibi Monocline	36.215287	-110.236693	6322	Dakota
27	WM10R-51A	Cotton Wood	36.074799	-109.888619	6067	Alluvial

Laboratory Analysis

Water samples were filtered using a 0.40 µm syringe filter into 50-mL polypropylene centrifuge tubes, and then pipetted into a 2-mL auto–sampler vials for analysis. Samples were analyzed using the Los Gatos Research (LGR) liquid water isotope analyzer (T-LWIA-45-EP; model: 912-0050-0001). Samples were injected ten times, discarding the first four to remove memory effects and averaging the last six injections. In-house water standards were used to correct the data to the VSMOW-SLAP scale. Reproducible injection sizes minimized the water concentration dependence of the analyzer, but a small correction was made using the USGS LIMS post-processing software. Analytical precision for repeated quality control samples was better than 0.2‰ for $\delta^{18}O$ and 1.0‰ for δD. Values for stable O and H are reported in delta notation per mil (‰) relative to VSMOW (Vienna Standard Mean Ocean Water).

Results

Precipitation amounts and stable isotopes.

Precipitation data for Oraibi Wash are shown in Table 3.5. Precipitation results collected in this project for the Oraibi watershed fluctuates with season. Greater amounts occurred during the winter months (December to March) compared to summer months (June to October). In the summer months, little to no precipitation was collected in the lower elevations near the outlet of Oraibi Wash. Greater precipitation were collected along the edge of the escarpment at higher elevations where trees, shrubs, and brushes grow. Previous research showed that winter precipitation amounts increase in mountain regions and summer monsoon provides most of the total annual precipitation in lower elevations including valleys and canyon bottoms (Tulley-Cordova et al., 2021).

Table 4 – Cumulative precipitation amounts in inches. Note: Snow amounts are reported as snow-water equivalent consistent with rain amounts.

Site #	Site ID	Total Precip.	Aug. 2018	Oct. 2018	Dec. 2018	Mar. 2019	Jun. 2019	Oct. 2019
1	WRV-P01	31.75	4.42	3.49	3.39	8.98	7.19	4.27
2	WPV-P01	21.99	4.27	2.62	3.00	3.96	2.17	5.97
3	BRW-P01	35.77	4.24	3.94	5.29	9.02	9.26	4.02
4	HRV-P01	21.09	3.84	3.36	3.36	3.80	3.48	3.27
5	IR-41-P01	25.91	1.90	4.67	4.50	7.52	2.84	4.47
6	JUA-P01	21.98	3.72	2.07	5.11	5.46	3.98	1.64
7	JUA-P02	18.67	0.34	1.72	5.65	6.47	3.53	0.96
8	HRC-P01	16.61	0.00	0.00	4.85	5.06	3.87	2.83
9	TL-P01	16.84	2.05	3.63	3.15	3.69	2.32	2.00
10	TL-P02	11.36	0.01	0.00	3.34	3.29	2.78	1.92

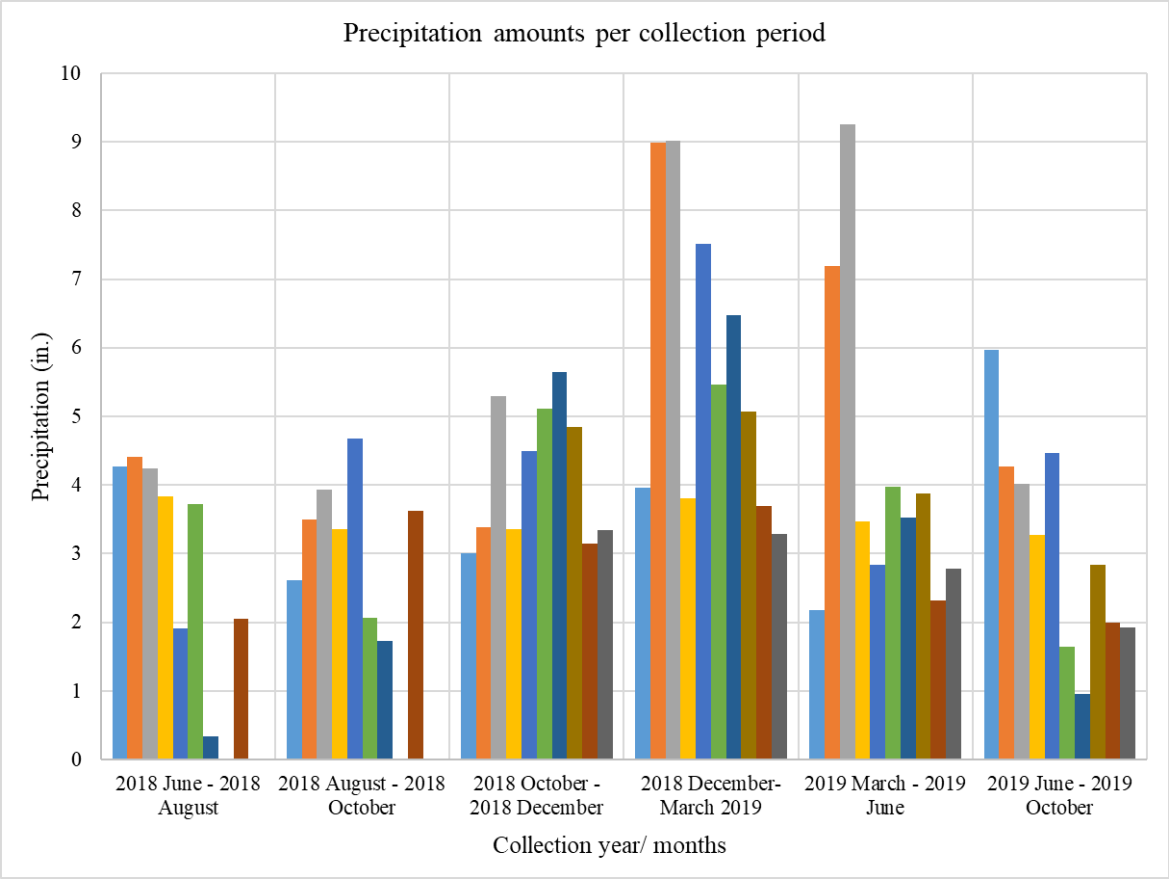

Figure 12 - Precipitation amounts collected within Oraibi Wash, AZ.

The isotopic values from precipitation that were sampled within the Oraibi watershed are presented in Figure 3.3. The $^{18}O/^{16}O$ and $^{2}H/1H$ ratios are expressed in delta notation using the equation (Rsample/Rstandard -1) * 1000 as permil (‰) values. The Local Meteoric Water Line (LMWL) was created using precipitation values of δD and $\delta^{18}O$ from the entire record of June 2018 to October 2019. Using the regression sum of squares method, the LMWL has a slope of 7.60 and y-intercept of 5.29 (R2=.98). Winter samples collected from December to March had the lightest isotopes ranging from -120 to -150‰ in δD and -16 to -19‰ in $\delta^{18}O$ values. The summer monsoon season had the most enriched samples from June to August, between -75 to -20‰ in δD and -9 to -2‰ in $\delta^{18}O$. In the spring and fall, precipitation values are intermediate with August to October ranging from -90 to -60‰ in δD and -12 to -10‰ in $\delta^{18}O$ values and March to June ranging from -100 to -60‰ in δD and -13 to -10‰ in $\delta^{18}O$. Summer precipitation had a mean and standard deviation of -7.71 +/-2.32‰ in $\delta^{18}O$ and the winter precipitation mean and standard deviation was -14.88 +/-2.82‰ in $\delta^{18}O$ which are referred to as the seasonal end members later.

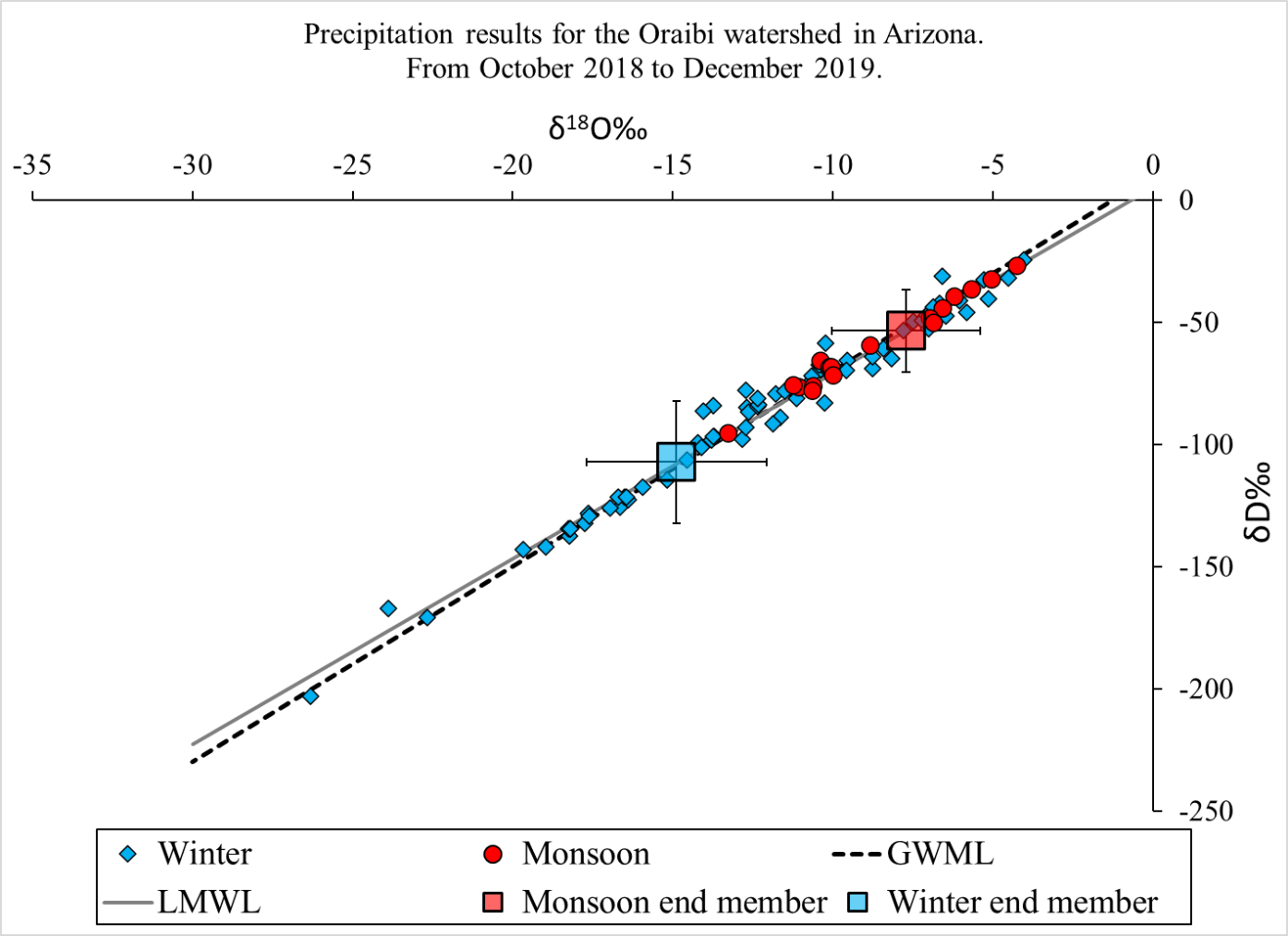

Figure 13 – Stable water isotopes in precipitation results with summer and winter end member values.

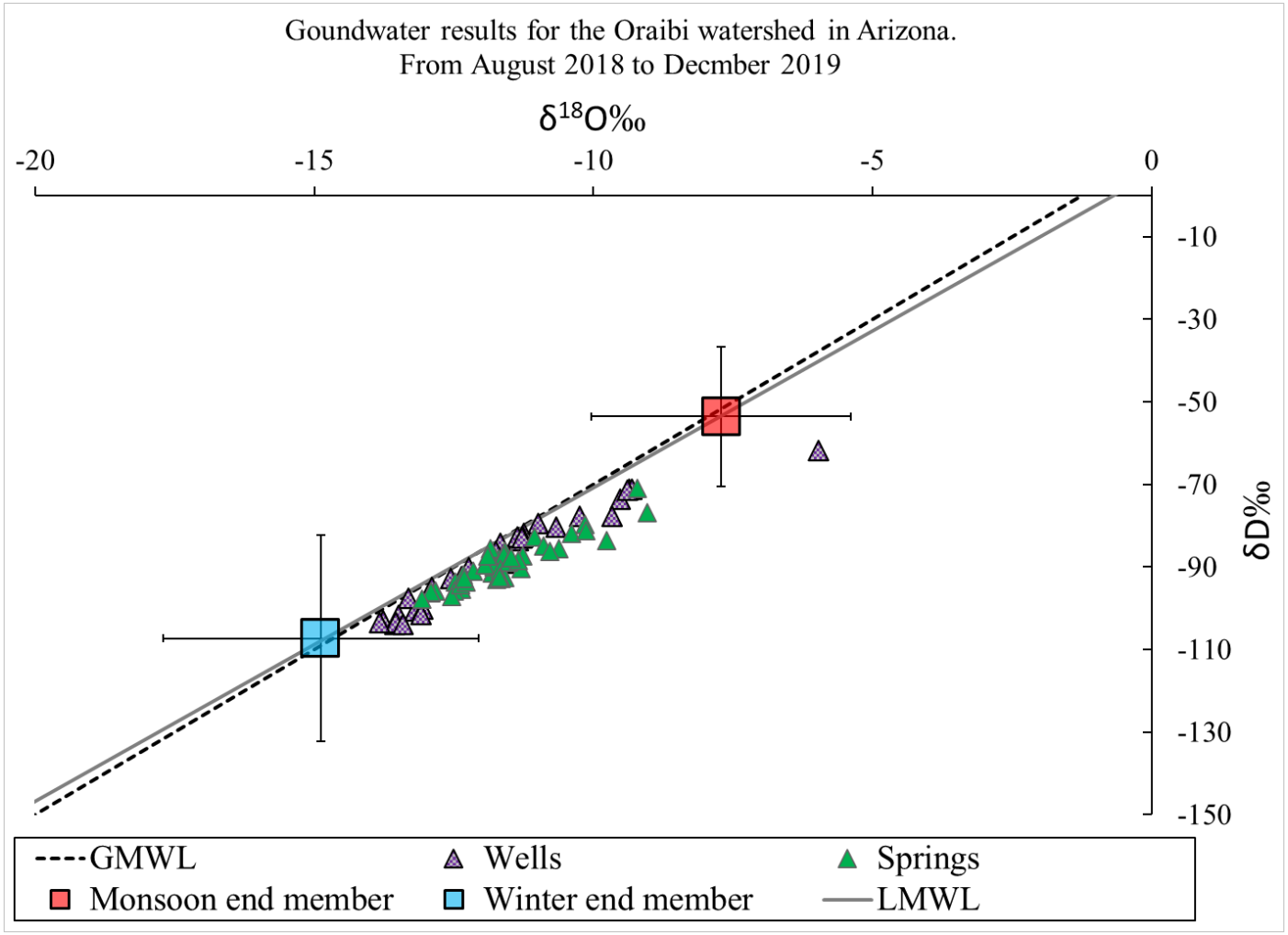

Figure 14 – Stable water isotope results for groundwater sampled from springs and wells and precipitation end member values.

Table 5 - Isotopic results for **springs** sampled from August 2018 to October 2019 in ‰.

Site #	Aug. 2018		Oct. 2018		Dec. 2018		Mar. 2019		Jun. 2019		Oct. 2019	
	δD	$\delta^{18}O$	δD	$\delta^{18}O$	δD	$\delta^{18}O$	δD	$\delta^{18}O$	δD	$\delta^{18}O$	δD	$\delta^{18}O$
28					-87.31	-11.26	-94.37	-12.38			-86.27	-10.78
29	-91.53	-11.82			-89.98	-11.78	-95.28	-12.36	-93.74	-12.28	-92.73	-12.31
30	-76.81	-9.04			-81.81	-10.39	-95.83	-12.49	-88.47	-11.35	-85.46	-10.62
31	-90.42	-11.30					-97.13	-12.54	-83.56	-9.76	-90.63	-11.67
32	-88.40	-11.82	-87.99	-11.70	-86.20	-11.59	-91.80	-12.34	-89.39	-11.95	-87.25	-11.90
33	-82.77	-11.06	-82.53	-11.84	-87.13	-11.60	-90.96	-12.15	-88.81	-11.53	-87.83	-11.48
34	-95.79	-12.84	-95.34	-12.42	-93.72	-12.47	-96.21	-12.92	-95.75	-12.83	-95.99	-12.92
35					-79.63	-10.15	-71.05	-9.22	-81.18	-10.13	-85.01	-10.89
36					-92.92	-11.73	-92.48	-11.59	-92.75	-11.65	-92.49	-11.68

Table 6 - Isotope results for **wells** sampled from August 2018 to October 2019.

Site #	Aug. 2018		Oct. 2018		Dec. 2018		Mar. 2019		Jun. 2019		Oct. 2019	
	δD	$\delta^{18}O$	δD	$\delta^{18}O$	δD	$\delta^{18}O$	δD	$\delta^{18}O$	δD	$\delta^{18}O$	δD	$\delta^{18}O$
21	-61.88	-5.97			-77.66	-9.67	-80.35	-10.67	-83.64	-11.34	-86.13	-11.76
22	-81.93	-11.25	-82.80	-11.26	-79.56	-10.99	-84.35	-11.66	-82.68	-11.36	-82.85	-11.29
23			-92.34	-12.37	-90.16	-12.24	-79.56	-10.99	-82.68	-11.36	-92.66	-11.29
24	-73.61	-9.53			-71.09	-9.35	-77.63	-10.24	-71.21	-9.31	-71.44	-9.40
25							-100.28	-13.06	-101.42	-13.09		
26	-103.96	-13.76	-103.05	-13.52	-99.48	-13.10	-89.02	-11.58	-101.74	-13.50	-103.47	-13.83
27			-103.96	-13.56	-100.61	-13.21	-103.28	-13.52	-103.53	-13.54	-103.92	-13.41

Partitioning summer and winter influence on groundwaters

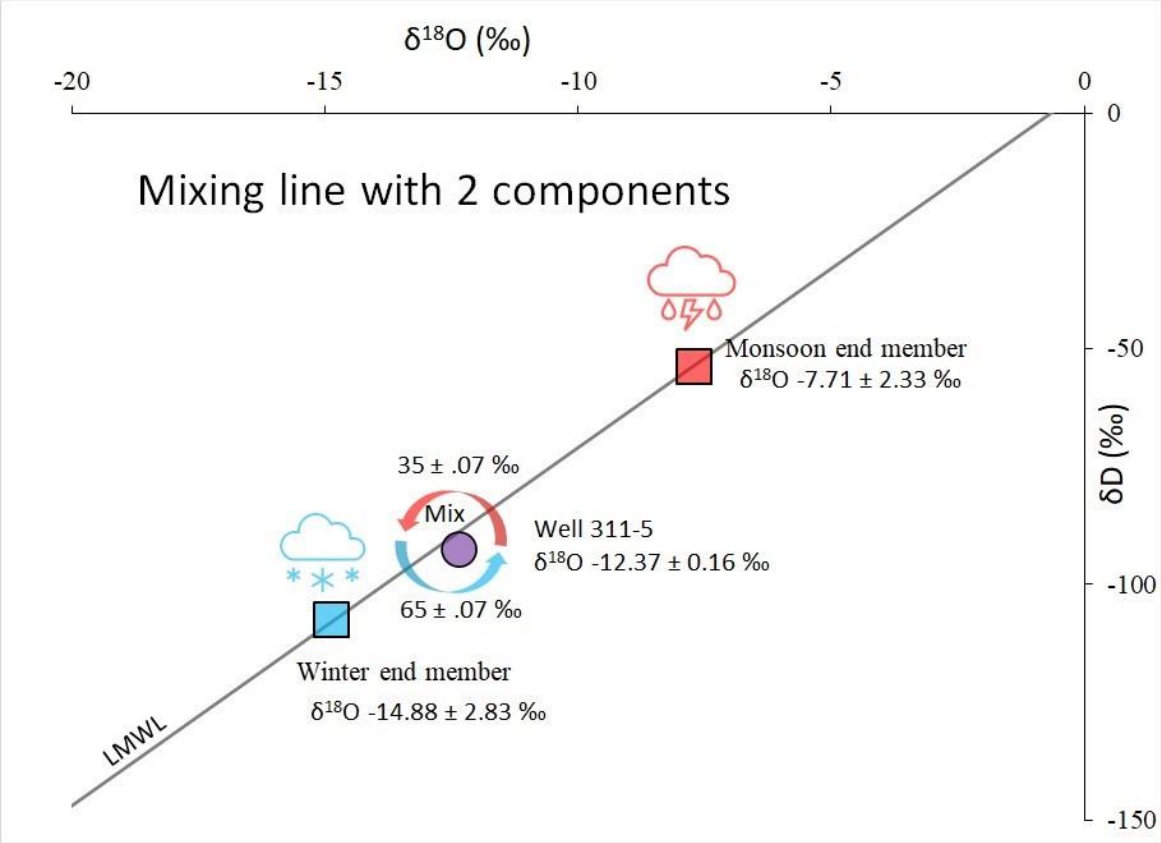

Figure 15 - Mixing model using stable water isotopes tracers in the water cycle.

The example in Figure 3.5 shows a mixing line with two components, δD and $\delta^{18}O$ described as end-members that are calculated from the average $\delta^{18}O$ summer and winter precipitation. These end-members are then used to calculate the fraction of winter and summer contribution to recharging groundwater from the Oraibi Wash precipitation samples. The closer the mix (groundwater sample) is to either end-member, the more likely the groundwater is recharged by winter or summer precipitation. The isotope composition of water is expressed as a ratio from heavy to light isotopes upon agreements of the Vienna-Standard mean Ocean water or VSMOW which was explain earlier in the laboratory analysis. Uncertainty was estimated using the Phillips and Gregg (2001) propagation of the measurement and end-member standard errors. Uncertainty in the end-member values is a larger source than analytical uncertainty.

Table 7 - Partitioning results for springs. W % means percent of winter recharge. Uncertainty represents the 95% confidence interval.

Site#	Aug. 2018		Oct. 2018		Dec. 2018		Mar. 2019		Jun. 2019		Oct. 2019	
	$\delta^{18}O$	W %	$\delta^{18}O$	W %	$\delta^{18}O$	W %	$\delta^{18}O$	W %	$\delta^{18}O$	W %	$\delta^{18}O$	W %
28					-11.26	50 ± 9.9	-12.38	65 ± 11.8			-10.78	43 ± 9.3
29	-11.82	57 ± 10.8			-11.78	57 ± 10.7	-12.36	65 ± 11.7	-12.28	64 ± 11.6	-12.31	64 ± 11.6
30	-9.04	19 ± 8.7			-10.39	37 ± 9.0	-12.49	67 ± 12.0	-11.35	51 ± 10.0	-10.62	41 ± 9.2
31	-11.30	50 ± 10.0			-11.67	55 ± 10.5	-12.54	67 ± 12.1			-9.76	29 ± 8.6
32	-11.82	57 ± 10.8	-11.70	56 ± 10.6	-11.59	54 ± 10.4	-12.34	65 ± 11.7	-11.95	59 ± 11.0	-11.90	58 ± 10.9
33	-11.06	47 ± 9.7	-11.84	58 ± 10.8	-11.60	54 ± 10.4	-12.15	62 ± 11.4	-11.53	53 ± 10.3	-11.48	53 ± 10.2
34	-12.84	72 ± 12.7	-12.42	66 ± 11.9	-12.47	66 ± 12.0	-12.92	73 ± 12.9	-12.83	71 ± 12.7	-12.92	73 ± 12.9
35					-10.15	34 ± 8.8	-9.22	21 ± 8.6	-10.13	34 ± 8.8	-10.89	44 ± 9.4
36					-11.73	56 ± 10.6	-11.59	54 ± 10.4	-11.65	55 ± 10.5	-11.68	55 ± 10.5

Table 8 - Partitioning results for wells W % means percent of winter recharge. Uncertainty represents the 95% confidence interval.

Site#	Aug. 2018		Oct. 2018		Dec. 2018		Mar. 2019		Jun. 2019		Oct. 2019	
wells	$\delta^{18}O$	W %	$\delta^{18}O$	W %	$\delta^{18}O$	W %	$\delta^{18}O$	W %	$\delta^{18}O$	W %	$\delta^{18}O$	W %
21	-5.97	-24 ± 13.0			-9.67	27 ± 8.6	-10.67	41 ± 9.2	-11.34	51 ± 10	-11.76	56 ± 10.7
22	-11.25	49 ± 9.9	-11.26	49 ± 9.9	-10.99	46 ± 9.6	-11.66	55 ± 10.5	-11.36	51 ± 10.1	-11.29	50 ± 10
23			-12.37	65 ± 11.8	-12.24	63 ± 11.5	-13.32	78 ± 13.7	-12.89	72 ± 12.8	-12.55	68 ± 12.1
24	-9.53	25 ± 8.6			-9.35	23 ± 8.6	-10.24	35 ± 8.9	-9.31	22 ± 8.6	-9.40	24 ± 8.6
25							-13.06	75 ± 13.1	-13.09	75 ± 13.2		
26	-13.76	84 ± 14.7	-13.52	81 ± 14.1	-13.10	75 ± 13.2	-11.58	54 ± 10.4	-13.50	81 ± 14.1	-13.83	85 ± 14.7
27			-13.56	82 ± 14.2	-13.21	77 ± 13.5	-13.52	81 ± 14.1	-13.54	81 ± 14.2	-13.41	80 ± 13.9

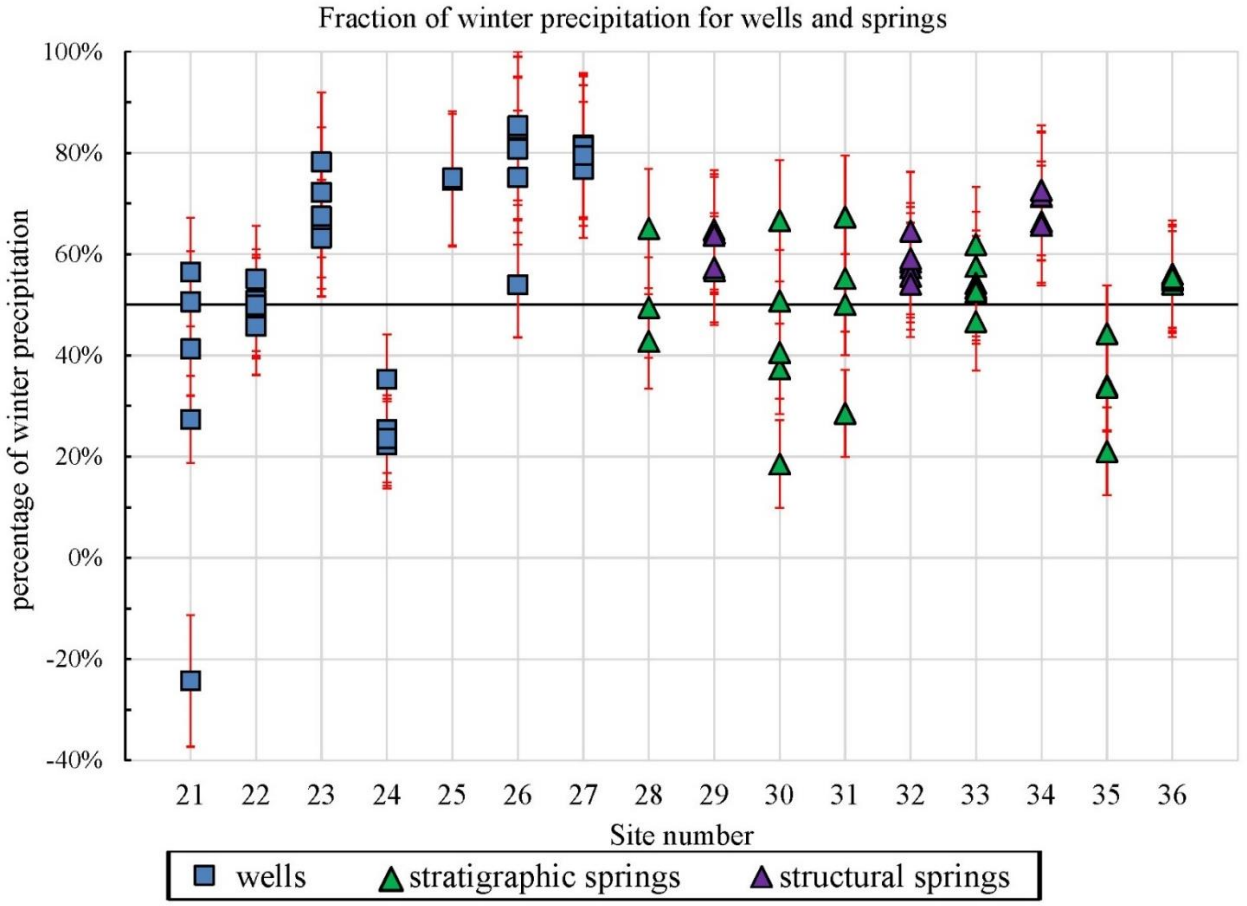

Figure 16 - Isotopic partitioning results for wells and springs for each sampling event plotted as the percentage of winter precipitation contributing to recharge. The vertical spread indicates seasonal variability in the stable water isotopic values at the site. Note: the negative value in site 21 is due to evaporation from an open holding tank causing isotopic enrichment. In this figure, the error bars represent the 95% confidence interval.

Springs

Springs samples have δD and $\delta^{18}O$ ratios between -97‰ to -71‰ and -12‰ to -9‰ (Table 3.5). On average, spring samples collected in March 2019 have the most isotopic ratios corresponding to the highest winter contributions. August 2018 and October 2019 had the most enriched isotopic ratios. In the Yale Point Sandstone are perennial seeps labeled 29 and 30, the isotope partitioning range is between 57% to 65% and 19% to 67%, respectfully of winter precipitation recharge. The highest winter contributions were in March 2019 (Table 3.7).

In the Wepo Formation sites 28 and 31 are two intermittent seeps that do not flow year around, the isotope partitioning range is between 43% to 65% and 29% to 67% of it being recharge from winter precipitation and the highest winter contributions in March 2019 (Table 3.7).

In the Toreva Formation are four perennial seeps labeled 33, 35, and 36. The isotope partitioning range is between 47% to 58%, 21% to 44%, and 54% to 56% of it being recharge from winter precipitation and the highest winter contributions in March 2019, October 2019, and December 2019. Spring 32 and 34 have a hydrostatic head of about 0.127 to 2.54 cm and 5.08 to 7.62 cm (between 0.5 – 3 in.), respectively. The isotope partitioning for winter precipitation recharge ranges between 54% to 65% for spring 32 and 66% to 73% for spring 34. The highest winter contribution was seen in March 2019 sample (Table 3.7).

The structure-controlled springs (labeled 29, 32, and 34 in Figure 16) had less isotopic variability and hence, less seasonal spread in estimated winter recharge fractions. Stratigraphically control springs (labeled 28, 30, 31, 33, and 35 in Figure 16) have a wider seasonal range in estimated winter recharge fractions.

Wells

Isotopic ratios sampled from wells that have enclosed storage tanks range from -103‰ to -71‰ δD and -13‰ to -9.2‰ $\delta^{18}O$ (Table 3.6). Many of the wells sampled suffered from evaporation in the holding tanks so we present here the lightest values measured for each well to minimize the evaporation influence. We acknowledge that the true groundwater isotopic values may change seasonally, however, the evaporation influence is likely the biggest driver of the sampling variability based on deuterium excess values. Therefore, we use the lightest isotopic values sampled from the holding tanks as the closest estimates of unevaporated groundwater.

Well 27 is in the alluvium and in October 2018, 82% was the highest percentage of this well recharged by winter precipitation. Other wells in the Toreva Formation included well 21. This well has a new closed storage tank installed in June 2019. The data points, therefore, are not comparable to the groundwater ratios shown in wells 22 to 27 even though all three wells are in the Toreva Formation. For well 21, the highest percentage result is from the October 2019 sample that has a value of 56%. For well 22 the highest winter partitioning result is at 55% from the March 2019. Well 24 isotopic winter partitioning result is at 35% with the highest percentage in March 2019.

Well 23 is the only well sourced from the Mancos Shale, the highest percentage in this well was recorded at 78% in the March 2019 sample. Well 26 is producing groundwater from the Dakota Sandstone, its highest isotopic partitioning result is 85% in the August 2019 sample.

Discussion

Comparison between the wells and springs relative to stratigraphic positions

The wells in Oraibi Wash produce from a range of different stratigraphic positions and we see clear differences in the source of groundwater recharge from different stratigraphic levels. Well 27, for example, produces groundwater from the Alluvium and has isotope partition values that tightly group between 77% to 82% (Figure 3.5). These high values represent a strong contribution of recharge from winter precipitation. The highest percentage is in October 2018 sample and the lowest percentage in December 2018. This is consistent with winter precipitation being concentrated between the months of October and March (Eastoe and Williams, 2019). In contrast, wells in the Toreva Formation have less winter contributions ranging from 56% to 35%. The four wells sourced from groundwater in stratigraphic units below the Toreva Formation, including the Mancos, Navajo, and Dakota Formations (23, 25, 26) have an average value greater than 60% (Figure 3.5). We interpret values from all these wells to reflect a strong component of recharge from winter precipitation but as noted there are some differences between individual formations.

Data collected from the springs, in contrast, show a stronger seasonality component of recharge compared to the wells. Springs in the upper watershed located above the stratigraphic position of the Toreva Formation (Figure 3.5; 28,30,31), for example, show a greater range of values. Springs where we documented a hydrostatic head during collection in the field, show less

seasonality with a tighter cluster value than the other springs. We interpret this difference to be related to these springs being sourced from deeper aquifers. These springs have values close to wells that are producing from deeper stratigraphic horizon such as the Mancos Shale (well 23). Although the Mancos Shale is considered a confining unit in most places.

Comparison of springs with structure and stratigraphic controls

When we compare the springs that emerge due to structural controls (fractures) to the springs that emerge due to stratigraphic controls (at the interface of layers with different permeability), we find that the spread in isotopic values and inferred winter recharge contributions are narrower in the structure-controlled springs 29,32, and 34 (Figure 16). Also, they do not show as much summer monsoon influence. Potential reasons included larger storage volumes (mixing) in the structure-controlled springs which dampen the seasonal variability and short and flashy monsoon events which do not allow for recharge in the fractured controlled zones.

Seasonal recharge implications

Springs and wells samples both clearly show the importance of winter precipitation recharge. This might be explained by comparing seasonal variations in winter and monsoon events. The summer monsoon precipitation events, for example, are often large downpours that lead to high velocity surface discharge in washes and canyons that leave little time for infiltration into subsurface aquifers. Winter precipitation, in contrast, accumulates at higher elevation in the headwaters of the washes, and slowly infiltrates subsurface aquifers and fractures along Oraibi Wash. In addition, shorter days in the winter lower evapotranspiration rates compared to the longer days of summer, thus leaving more precipitation available for groundwater recharge.

However, it is important to note that the spring samples show a greater seasonality with a mixture of winter and monsoon precipitation. This can be seen in the wider range of values in springs indicating a component of monsoon precipitation. This is clear, for example, where we have springs that are located directly next to wells but have different isotopic composition suggesting different sources of recharge.

Conclusions

1) The communities located within the Colorado River watershed are dealing with one of the most severe droughts in U.S. history. Recent public media have published many accounts of both the demise of the Colorado River, and the reservoirs along the river that supply drinking water and electricity throughout the southwestern U.S. Indigenous communities in this watershed utilize surface and groundwater as a resource for drinking water and agriculture. These Native communities also consider the Colorado River sacred with the river being deeply ingrained into their culture and ceremonies.

2) To better understand the sources of groundwater recharge on the Navajo reservation and how these changes in sources might be impacted by climate change, this study focuses on sources of groundwater recharge along Oraibi Wash. This drainage is in Black Mesa, Arizona in the heart of the Navajo and Hopi reservations and is a tributary of the Little Colorado River. Analysis of water samples from wells and springs along Oraibi Wash have identified the importance of winter precipitation for groundwater recharge as defined through stable isotope measurements. Water samples collected from wells, for example, plot closer to the winter endmember of precipitation. This finding emphasizes the importance of the deeper aquifers being recharged from winter precipitation. The data from the deeper aquifers are interpreted to reflect the regional sources of groundwater recharge and point to the importance of winter precipitation throughout the regional watershed. Another aspect may be that the deeper wells are located directly in the valley of Oraibi Wash. These valleys contain thick sections of unconsolidated sand and gravel that we hypothesize may provide a direct connection for recharging the deeper aquifers by winter precipitation. In this framework, winter precipitation is transported through the sand and gravel of the alluvial like a sponge creating a flow path to deeper aquifers.

3) Isotopic measurements of spring waters along Oraibi watershed showed seasonal variability, indicating sensitivity to both winter snowmelt and summer monsoon recharge. The flow paths for these springs are through sedimentary strata that make up the bedrock of Oraibi Wash. Precipitation enters these strata through vertical fractures and then migrates downdip through porous strata until forming a spring where the aquifer intersects the canyon walls of Oraibi

Wash. This direct near-surface connection to both summer and winter precipitation makes these springs sensitive to seasonality and vulnerable to long-term changes in local precipitation.

4) The seasonal variability in the stable water isotopic values of the springs was reduced for springs controlled by geologic structure compared to stratigraphic control. Possibilities for these differences include larger groundwater storage volumes in the structure control springs or less monsoon infiltration in the structure-controlled recharge zones.

5) Implications for these new findings indicate that winter recharge of groundwater will be critical for Navajo communities along Oraibi Wash. Changes in precipitation due to climate change that impact winter precipitation will have profound effects on groundwater in Oraibi Wash, and consequently, also on the Native communities living along this drainage.

Reference

Clark, Ian D., and Fritz, Peter. *Environmental Isotopes in Hydrogeology*. 0 ed. CRC Press, 2013. https://doi.org/10.1201/9781482242911.

Earman, S., A. R. Campbell, F. M. Phillips, and B. D. Newman (2006), Isotopic exchange between snow and atmospheric water vapor: Estimation of the snowmelt component of groundwater recharge in the southwestern United States, J. *Geophys. Res*.,111,D09302, doi:10.1029/2005JD006470.

Eastoe, C. J., & Wright, W. E. (2019). Hydrology of mountain blocks in Arizona and New Mexico as revealed by isotopes in groundwater and precipitation. Geosciences, 9, 461. https://doi.org/10.3390/geosciences9110461

Genereux, D. (1998). Quantifying uncertainty in tracer-based hydrograph separations. Water Resources Research, 34(4), 915-919.

González-Trinidad, J., Pacheco-Guerrero, A., Júnez-Ferreira, H., Bautista-Capetillo, C., & Hernández-Antonio, A. (2017). Identifying groundwater recharge sites through environmental stable isotopes in an alluvial aquifer. Water, 9(8), 569.

Jana, S., Rajagopalan, B., Alexander, M.A., & Ray, A. J. (2018). Understanding the dominant sources and tracks of moisture for summer rainfall in the southwest United States. Journal of Geophysical Research: Atmospheres,123,4850–4870. https://doi.org/10.1029/2017JD027652.

Jasechko, Scott, S. Jean Birks, Tom Gleeson, Yoshihide Wada, Peter J. Fawcett, Zachary D. Sharp, Jeffrey J. McDonnell, and Jeffrey M. Welker. "The Pronounced Seasonality of Global Groundwater Recharge." *Water Resources Research* 50, no. 11 (November 2014): 8845–67. https://doi.org/10.1002/2014WR015809.

Phillips, D. L., & Gregg, J. W. (2001). Uncertainty in source partitioning using stable isotopes. Oecologia, 171-179.

Simpson, E.S., Thorrud, D.B., and Friedman, Irving, 1970, Distinguishing seasonal recharge to goundwater by deuterium analysis in southern Arizona (with discussion): International Association of Scientific Hydrology Publication.

Solder, John E., and Kimberly R. Beisner. "Critical Evaluation of Stable Isotope Mixing End-Members for Estimating Groundwater Recharge Sources: Case Study from the South Rim of the Grand Canyon, Arizona, USA." *Hydrogeology Journal* 28, no. 5 (August 2020): 1575–91. https://doi.org/10.1007/s10040-020-02194-y.

Tsinnajinnie, L. M., Gutzler, D. S., & John, J. (2018). Navajo Nation snowpack variability from 1985 to 2014 and implications for water resources management. Journal of Contemporary Water Research & Education, 163, 124–138. https://doi.org/10.1111/j.1936-704X.2018.03274.x

Tsinnajinnie, L. 2011. An Analysis of Navajo Nation Snow Courses and Snowpack Data in the Chuska Mountains. Water Resources Professional Projects Report. Available at: http://digitalrepository.unm.edu/wr_sp/49/.

Tulley-Cordova, C.L., Strong, C., Brady, I.P., Bekis, J. and Bowen, G.J. (2018), Navajo Nation, USA, Precipitation Variability from 2002 to 2015. Journal of Contemporary Water Research & Education, 163: 109-123. https://doi.org/10.1111/j.1936-704X.2018.03273.x

Redsteer, M. H., Kelley, K. B., Francis, H., & Block, D. (2010). Disaster risk assessment case study: Recent drought on the Navajo nation, southwestern United States. In *2011 global assessment report on disaster risk reduction* (pp. 1-19). Geneva, Switzerland: United Nations Office for Disaster Risk Reduction.

Redsteer, M. H., 2011: Increasing Vulnerability to Drought and Climate Change on the Navajo Nation, Southwestern United States. Current Conditions & Accounts Of Changes During The Last 100 Years. 31 pp., U.S. Geological Survey. 0928.

Winograd, I. J., Riggs, A.C., Coplen, T.B., The relative contributions of summer and cool-season precipitation to groundwater recharge, Spring Mountains, Neveada, USA. Hydrogeology Journal. 6 (1998), pp. 77-93, 10.1007/s1004000050135

Zamora, H.A.; Eastoe, C.J.; Wilder, B.T.; McIntosh, J.C.; Meixner, T.; Flessa, K.W. Groundwater Isotopes in the Sonoyta River Watershed, USA-Mexico: Implications for Recharge Sources and Management of the Quitobaquito Springs. Water 2020, 12, 3307. https://doi.org/10.3390/w12123307

APPENDIX A: EARTHEN DAMS

Sample ID	Collection Date	Analysis Date	δD Mean	δD StDev	$\delta^{18}O$ Mean	$\delta^{18}O$ StDev	Deuterium excess	Mean H_2O	Latitude	Longitude	Elevation meters
ED-01	8/8/18 12:28	9/14/18 20:31	10.5	0.45	5.14	0.10	-30.65	3.58	36.15427	-110.35338	1867
ED-01-02	10/6/2018 19:04	12/14/2018 20:59	-100.37	0.55	-13.017	0.055	3.766	3.90	36.15427	-110.35338	1867
ED-01-03	12/17/2018 16:20	2/3/2019 20:26	-72.69	0.25	-8.54	0.02	-4.36	4.14	36.15427	-110.35338	1867
ED-01-04	3/9/2019 18:42	3/29/2019 23:36	-81.04	0.62	-9.21	0.04	-7.34	3.96	36.15427	-110.35338	1867
ED-07	8/13/18 14:03	9/14/18 23:06	-5.95	0.36	1.53	0.06	-18.21	3.55	36.21233	-110.24345	1924
ED-07-03	12/23/2018 12:02	2/3/2019 23:14	-72.63	0.16	-9.57	0.08	3.91	4.13	36.21233	-110.24345	1924
ED-07-04	3/13/2019 14:49	3/28/2019 23:23	-97.51	0.61	-12.85	0.15	5.31	4.05	36.21233	-110.24345	1924
ED-02	8/9/18 13:10	9/14/18 20:47	1.48	0.24	4.79	0.11	-36.84	3.52	36.30392	-110.12598	1984
ED-02-03	12/23/2018 12:48	2/3/2019 20:42	-39.71	0.20	-2.23	0.05	-21.90	4.11	36.30392	-110.12598	1984
ED-02-04	3/13/2019 14:10	3/29/2019 23:51	-91.91	0.53	-12.21	0.10	5.77	3.96	36.30392	-110.12598	1984
ED-03	8/9/18 13:42	9/14/18 22:04	15.79	0.34	4.72	0.05	-21.99	3.54	36.31839	-110.10152	1994
ED-03-03	12/18/2018 12:25	2/6/2019 20:01	-48.95	0.16	-4.40	0.08	-13.73	4.06	36.31839	-110.10152	1995
ED-03-04	3/13/2019 13:35	3/28/2019 20:35	-110.36	0.35	-14.46	0.05	5.32	4.03	36.31839	-110.10152	2007
ED-03-05	6/20/2019 11:33	9/16/2019 00:50	27.84	0.92	14.93	0.12	-91.56	4.13	36.31839	-110.10152	2007
ED-08	8/14/18 16:49	9/15/18 0:08	-21.31	0.27	-0.16	0.08	-20.00	3.58	36.34402	-110.06152	2036
ED-08-03	12/21/2018 15:26	2/3/2019 23:30	-34.73	0.28	-1.82	0.08	-20.16	4.11	36.34402	-110.06152	2036
ED-08-04	3/10/2019 14:20	3/29/2019 00:40	-109.13	0.32	-14.45	0.10	6.44	4.06	36.34402	-110.06152	2036
ED-08-05	6/20/2019 12:25	9/16/2019 02:37	13.27	0.53	9.81	0.11	-65.22	3.97	36.34402	-110.06152	2036
ED-08-06	10/11/2019 12:26	12/19/2019 22:43	31.35	0.51	9.60	0.07	-45.41	3.59	36.34402	-110.06152	2036
ED-06	8/11/18 15:45	9/14/18 22:51	-29.91	0.18	-1.87	0.11	-14.97	3.54	36.37699	-110.07406	2050
ED-06-02	10/7/2018 15:45	12/22/2018 05:52	26.91	0.7	9.948	0.092	-52.674	3.82	36.37699	-110.07406	2050
ED-06-03	12/19/2018 15:26	2/3/2019 22:59	19.60	0.24	8.39	0.09	-47.49	4.10	36.37699	-110.07406	2050

ED-06-04	3/11/2019 15:16	3/28/2019 23:08	-92.32	0.41	-10.77	0.09	-6.14	4.02	36.37699	-110.07406	2050
ED-06-05	6/20/2019 17:40	9/16/2019 01:20	-72.69	0.71	-6.92	0.12	-17.32	4.16	36.37699	-110.07406	2050
ED-06-06	10/11/2019 15:40	12/19/2019 22:27	-37.56	0.33	-0.73	0.12	-31.70	3.62	36.37699	-110.07406	2050
311-5-ED	10/7/2018 14:17	12/14/2018 21:14	-18.65	0.58	0.205	0.107	-20.29	3.90	36.40056	-110.11574	2086
311-5-ED	12/23/2018 14:31	2/3/2019 20:57	-33.69	0.18	-2.44	0.09	-14.15	4.12	36.40056	-110.11574	2086
311-5-ED-04	3/10/2019 19:57	3/28/2019 22:37	-98.87	0.38	-12.98	0.07	4.98	4.05	36.40056	-110.11574	2086
ED-05	8/12/18 15:00	9/14/18 22:35	36.56	0.57	12.55	0.16	-63.81	3.55	36.41096	-110.06815	2110
ED-05-03	12/20/2018 14:15	2/3/2019 22:44	18.31	0.16	8.50	0.05	-49.70	4.10	36.41096	-110.06815	2110
ED-05-04	3/11/2019 12:03	3/28/2019 22:52	-114.01	0.39	-14.94	0.06	5.51	4.05	36.41096	-110.06815	2110
ED-05-05	6/16/2019 08:30	9/16/2019 01:05	-73.53	0.84	-6.43	0.13	-22.12	4.14	36.41096	-110.06815	2110
ED-05-06	10/11/2019 14:45	12/19/2019 22:12	-2.09	0.25	8.06	0.10	-66.53	3.63	36.41096	-110.06815	2110
4T-500-ED-04	3/14/2019 12:46	3/29/2019 00:55	-103.73	0.39	-14.00	0.10	8.27	4.04	36.34303	-109.93427	2139
ED-04-04	3/10/2019 12:31	3/28/2019 22:22	-105.83	0.68	-14.44	0.12	9.71	4.06	36.34204	-109.88436	2211
ED-04-06	10/11/2019 11:31	12/19/2019 21:56	-48.30	0.61	-5.14	0.07	-7.16	3.70	36.34204	-109.88436	2211
ED-04	8/9/18 17:37	9/14/18 22:20	31.34	0.37	11.41	0.06	-59.93	3.57	36.34204	-109.88436	2211

APPENDIX B: STEM PLANT DATA

Sample ID	Collection Date	Analysis Date	Mean [H_2O]	$\delta^{18}O$ Mean	$\delta^{18}O$ StDev	L1 Narrow Band Metric	L1 Broad Band Metric	$\delta^{18}O$ Final Corrected	Latitude	Longitude	Elevation meters	Aspect	Other Information
3C-01-0619	6/14/19 17:57	3/4/48 0:00	3.82E+16	-6.87	0.11	196.07	1.19	-10.55	36.216	-110.24544	1918	East	Tamarisk shrub
3C-01-1019	10/6/19 19:11	3/4/48 0:00	3.92E+16	-1.44	0.15	1441.80	1.01	-9.08	36.216	-110.24544	1918	East	Tamarisk shrub
3C-01-1218	12/17/18 17:14	3/4/48 0:00	3.94E+16	-4.43	0.17	1.48	1.00	-4.14	36.216	-110.24544	1918	East	Tamarisk shrub
AE-01-0619	6/14/19 18:16	3/4/48 0:00	3.64E+16	13.99	0.16	69489.20	1.23	-9.81	36.21151	-110.24773	1906	West	American Elm Tree
AE-01-1019	10/6/19 18:47	3/4/48 0:00	3.37E+16	-6.17	0.98	54.52	1.66	-6.25	36.21151	-110.24773	1906	West	American Elm Tree
ASV-01-0319	3/10/19 19:20	3/4/48 0:00	3.66E+16	-4.79	0.20	1.92	1.33	-3.54	36.4396	-110.08082	2148	East	Gambel Oak tree
ASV-01-0619	6/15/19 18:34	3/4/48 0:00	3.72E+16	-4.32	0.18	2720.67	1.23	-13.07	36.4396	-110.08082	2148	East	Gambel Oak tree
ASV-01-1019	10/8/19 15:36	3/4/48 0:00	3.78E+16	-10.50	0.26	75.59	1.01	-13.73	36.4396	-110.08082	2148	East	Gambel Oak tree
ASV-03-0619	6/15/19 18:36	3/4/48 0:00	3.83E+16	-13.08	0.03	1.98	1.00	-12.95	36.43989	-110.08047	2168	South	Gambel Oak tree
ASV-03-1019	10/8/19 15:37	3/4/48 0:00	3.70E+16	-5.60	0.10	235.41	1.01	-10.31	36.43989	-110.08047	2168	South	Gambel Oak tree
ASV-03-1218	12/18/18 16:14	3/4/48 0:00	3.58E+16	-5.80	0.22	4.86	1.01	-6.07	36.43989	-110.08047	2168	South	Gambel Oak tree
BRW-01-0619	6/20/19 19:36	3/4/48 0:00	3.18E+16	-5.14	0.29	475.52	1.26	-10.78	36.40581	-110.16624	2250	North	Colorado Pinon Tree
BRW-01-1018	10/7/18 13:35	3/4/48 0:00	3.37E+16	-0.42	0.66	347.60	1.20	-5.62	36.40581	-110.16624	2250	North	Colorado Pinon Tree
BRW-01-1019	10/8/19 16:13	3/4/48 0:00	3.74E+16	-7.92	0.24	48.76	1.19	-10.19	36.40581	-110.16624	2250	North	Colorado Pinon Tree
BRW-01-1218	12/18/18 10:24	3/4/48 0:00	3.75E+16	-4.77	0.21	22.57	1.22	-6.19	36.40581	-110.16624	2250	North	Colorado Pinon Tree
BRW-03-0319	3/10/19 20:32	3/4/48 0:00	3.60E+16	-8.15	0.44	19.93	1.37	-8.75	36.41447	-110.15324	2151	North	Gambel Oak tree
BRW-03-0619	6/20/19 19:43	3/5/48 0:00	3.83E+16	-1.21	0.19	5021.99	1.24	-11.32	36.41447	-110.15324	2151	North	Gambel Oak tree
BRW-03-1018	10/7/18 13:47	3/5/48 0:00	3.95E+16	-5.10	0.09	79.42	1.00	-7.79	36.41447	-110.15324	2151	North	Gambel Oak tree
BRW-03-1019	10/8/19 15:33	3/5/48 0:00	3.93E+16	-11.56	0.16	84.75	1.00	-14.35	36.41447	-110.15324	2151	North	Gambel Oak tree
BSV-01-0319	3/10/19 18:00	3/5/48 0:00	3.82E+16	-8.16	0.06	22.78	1.24	-9.50	36.43972	-110.11374	2133	North	Rocky Mtn Juniper

BSV-01-0619	6/15/19 17:06	3/5/48 0:00	3.81E+16	-10.03	0.15	141.83	1.22	-13.13	36.43972	-110.11374	2133	North	Rocky Mtn Juniper
BSV-01-1019	10/8/19 13:37	3/5/48 0:00	3.86E+16	-8.75	0.07	156.15	1.20	-11.91	36.43972	-110.11374	2133	North	Rocky Mtn Juniper
BSV-01-1218	12/18/18 14:31	3/5/48 0:00	3.92E+16	-7.57	0.14	28.13	1.00	-9.41	36.43972	-110.11374	2133	North	Rocky Mtn Juniper
BSV-03-0319	3/10/19 17:59	3/5/48 0:00	3.93E+16	-6.02	0.12	40.32	1.10	-7.92	36.43906	-110.11512	2170	North	lodgepole pine (Pinus contorta)
BSV-03-0619	6/15/19 17:40	3/5/48 0:00	3.89E+16	2.98	0.05	3997.78	1.15	-6.51	36.43906	-110.11512	2170	North	lodgepole pine (Pinus contorta)
BSV-03-1019	10/8/19 13:45	3/5/48 0:00	3.93E+16	-10.53	0.11	9.44	1.00	-11.51	36.43906	-110.11512	2170	North	lodgepole pine (Pinus contorta)
BSV-03-1218	12/18/18 14:44	3/5/48 0:00	3.83E+16	2.25	0.15	2226.48	1.18	-5.68	36.43906	-110.11512	2170	North	lodgepole pine (Pinus contorta)
CT-01-0619	6/16/19 8:31	3/5/48 0:00	3.95E+16	-11.85	0.06	13.92	1.00	-13.10	36.41119	-110.0687	2105	South	Greasewood shrub
CT-01-1019	10/11/19 14:29	3/5/48 0:00	3.79E+16	-3.91	0.22	537.47	1.34	-8.63	36.41119	-110.0687	2105	South	Greasewood shrub
CT-02-0619	6/16/19 8:42	3/5/48 0:00	3.92E+16	0.98	0.09	8698.42	1.11	-11.16	36.41015	-110.0688	2097	South	Greasewood shrub
CT-02-1019	10/11/19 14:36	3/5/48 0:00	3.74E+16	-1.31	0.20	1431.29	1.36	-7.97	36.41015	-110.0688	2097	South	Greasewood shrub
HRV-01-0319	3/11/19 18:59	3/5/48 0:00	3.84E+16	-6.38	0.08	64.55	1.24	-8.54	36.33912	-110.08624	2030	West	Ponderosa Pine Tree
HRV-01-0619	6/20/19 14:43	3/7/48 0:00	3.80E+16	-4.20	0.04	770.62	1.22	-10.36	36.33912	-110.08624	2030	West	Ponderosa Pine Tree
HRV-01-1018	10/7/18 16:54	3/7/48 0:00	3.81E+16	-5.56	0.13	220.25	1.24	-9.60	36.33912	-110.08624	2030	West	Ponderosa Pine Tree
HRV-01-1019	10/11/19 16:32	3/7/48 0:00	3.86E+16	0.54	0.19	3620.26	1.13	-9.39	36.33912	-110.08624	2030	West	Ponderosa Pine Tree
HRV-01-1218	12/20/18 15:39	3/7/48 0:00	3.82E+16	1.79	0.08	1025.60	1.19	-4.98	36.33912	-110.08624	2030	West	Ponderosa Pine Tree
HRV-03-0319	3/11/19 18:48	3/7/48 0:00	3.78E+16	-6.21	0.11	130.55	1.33	-9.32	36.33865	-110.08726	2030	South	Colorado Pinon Tree
HRV-03-0619	6/20/19 14:48	3/7/48 0:00	3.71E+16	-9.33	0.14	44.75	1.43	-10.72	36.33865	-110.08726	2030	South	Colorado Pinon Tree
HRV-03-1019	10/11/19 16:49	3/7/48 0:00	3.82E+16	-6.11	0.14	195.23	1.20	-10.09	36.33865	-110.08726	2030	South	Colorado Pinon Tree
HRV-03-1218	12/20/18 15:45	3/7/48 0:00	3.76E+16	-5.50	0.18	51.86	1.35	-7.31	36.33865	-110.08726	2030	South	Colorado Pinon Tree
JUA-N01-0319	3/9/19 17:36	3/7/48 0:00	3.95E+16	-6.57	0.10	4.38	1.00	-6.43	36.09987	-110.42709	1820	East	Tamarisk shrub
JUA-N01-1218	12/17/18 14:31	3/7/48 0:00	3.80E+16	-4.09	0.09	284.45	1.30	-8.33	36.09987	-110.42709	1820	East	Tamarisk shrub
JUA-N03-0619	6/14/19 14:53	3/7/48 0:00	3.87E+16	9.74	0.08	34104.53	1.08	-9.17	36.09994	-110.42717	1819	North	Greasewood shrub

JUA-N03-1018	10/6/18 17:49	3/7/48 0:00	3.93E+16	-5.31	0.06	165.48	1.00	-9.16	36.09994	-110.42717	1819	North	Greasewood shrub
JUA-N03-1019	10/6/19 16:40	3/7/48 0:00	3.94E+16	-9.69	0.13	3.39	1.00	-9.56	36.09994	-110.42717	1819	North	Greasewood shrub
JUA-N05-0319	3/9/19 18:00	3/7/48 0:00	3.63E+16	-6.69	0.16	10.83	1.58	-5.66	36.09994	-110.42717	1819	South	Tamarisk shrub
JUA-N05-0619	6/14/19 16:03	3/7/48 0:00	3.86E+16	0.41	0.24	7576.49	1.10	-11.96	36.09994	-110.42717	1819	South	Tamarisk shrub
JUA-N05-1019	10/6/19 17:11	3/7/48 0:00	3.81E+16	-9.68	0.15	15.38	1.25	-9.34	36.09994	-110.42717	1819	South	Tamarisk shrub
JUA-N07-0319	3/9/19 18:03	3/10/48 0:00	3.70E+16	48.19	0.09	1030078.33	1.29	-1.37	36.12352	-110.39883	1818	South	Greasewood shrub
JUA-N07-0619	6/14/19 16:04	3/10/48 0:00	3.80E+16	32.18	0.19	605396.17	1.12	-11.06	36.12352	-110.39883	1818	South	Greasewood shrub
JUA-N07-0818	8/8/18 14:04	3/10/48 0:00	3.85E+16	17.11	0.11	64024.33	1.13	-5.78	36.12352	-110.39883	1818	South	Greasewood shrub
JUA-N09-0319	3/9/19 18:44	3/10/48 0:00	3.96E+16	-7.16	0.07	17.29	1.01	-8.23	36.15406	-110.3527	2017	South	Greasewood shrub
JUA-N09-0619	6/14/19 17:06	3/10/48 0:00	3.93E+16	-7.36	0.15	50.76	1.00	-9.61	36.15406	-110.3527	2017	South	Greasewood shrub
JUA-N09-1019	10/6/19 18:06	3/10/48 0:00	3.96E+16	-9.04	0.19	25.14	1.00	-10.52	36.15406	-110.3527	2017	South	Greasewood shrub
JUA-N09-1218	12/17/18 15:58	3/10/48 0:00	3.95E+16	-7.81	0.16	23.95	1.00	-9.26	36.15406	-110.3527	2017	South	Greasewood shrub
JUA-N11-0319	3/9/19 18:51	3/10/48 0:00	3.95E+16	-12.60	0.17	10.05	1.00	-13.20	36.15448	-110.35432	1865	East	Juniper tree
JUA-N11-0619	6/14/19 17:15	3/10/48 0:00	3.86E+16	-5.00	0.10	1797.83	1.14	-12.70	36.15448	-110.35432	1865	East	Juniper tree
LE-01-0319	3/13/19 13:40	3/10/48 0:00	3.96E+16	-6.60	0.08	18.35	1.00	-7.78	36.31859	-110.10102	1998	South	Greasewood shrub
LE-01-0619	6/20/19 11:22	3/10/48 0:00	3.87E+16	-0.45	0.11	2177.40	1.15	-8.60	36.31859	-110.10102	1998	South	Greasewood shrub
LE-01-1019	10/10/19 16:43	3/10/48 0:00	3.91E+16	-6.82	0.14	107.53	1.10	-9.52	36.31859	-110.10102	1998	South	Greasewood shrub

LE-03-0619	6/20/19 11:27	3/10/48 0:00	3.82E+16	-2.53	0.17	337.98	1.28	-6.32	36.31837	-110.10184	1993	South	Greasewood shrub
LE-03-1218	12/18/18 9:15	3/10/48 0:00	3.98E+16	-3.63	0.16	228.65	1.00	-7.64	36.31837	-110.10184	1993	South	Greasewood shrub
RC-01-0619	6/20/19 10:59	3/10/48 0:00	3.90E+16	-1.29	0.09	599.83	1.12	-6.59	36.30397	-110.12626	1988	North	Greasewood shrub
RC-01-1019	10/10/19 16:29	3/10/48 0:00	3.98E+16	-5.41	0.13	67.82	1.00	-7.87	36.30397	-110.12626	1988	North	Greasewood shrub
RC-03-0619	6/20/19 11:06	3/11/48 0:00	3.83E+16	-5.29	0.12	433.85	1.22	-9.59	36.30382	-110.12623	1988	South	Greasewood shrub
RC-03-1019	10/10/19 16:24	3/11/48 0:00	3.96E+16	-4.85	0.18	273.39	1.00	-9.08	36.30382	-110.12623	1988	South	Greasewood shrub
SD-01-0619	6/20/19 17:48	3/11/48 0:00	3.82E+16	3.50	0.13	1298.92	1.21	-3.03	36.37634	-110.07357	2032	South	Greasewood shrub
SD-01-1018	10/7/18 15:07	3/11/48 0:00	3.64E+16	-4.34	0.11	552.14	1.67	-7.57	36.37634	-110.07357	2032	South	Greasewood shrub
SD-01-1019	10/11/19 15:20	3/11/48 0:00	3.82E+16	-3.87	0.12	446.05	1.27	-8.02	36.37634	-110.07357	2032	South	Greasewood shrub
SD-01-1218	12/19/18 15:38	3/11/48 0:00	3.85E+16	4.62	0.16	732.59	1.24	-0.50	36.37634	-110.07357	2032	South	Greasewood shrub
SD-03-0619	6/20/19 17:59	3/11/48 0:00	3.92E+16	-0.52	0.15	3252.65	1.12	-9.62	36.37604	-110.07349	2038	South	Greasewood shrub
SPT-01-0619	6/15/19 15:30	3/11/48 0:00	3.90E+16	-8.07	0.11	153.67	1.15	-11.01	36.458	-110.152	2206	West	lodgepole pine (Pinus contorta)
SPT-01-1019	10/8/19 12:15	3/11/48 0:00	3.82E+16	-13.26	0.05	53.45	1.30	-14.52	36.458	-110.152	2206	West	lodgepole pine (Pinus contorta)
SPT-01-1218	12/18/18 12:58	3/11/48 0:00	3.96E+16	-7.01	0.14	112.47	1.00	-10.04	36.458	-110.152	2206	West	lodgepole pine (Pinus contorta)
SS-01A-0319	3/11/19 11:57	3/11/48 0:00	3.55E+16	6.96	0.09	1859.16	1.78	1.43	36.42211	-110.06901	2144	South	Rocky Mountain birch
SS-01A-0619	6/15/19 20:13	3/11/48 0:00	3.66E+16	37.59	0.12	463994.67	1.38	-2.21	36.42211	-110.06901	2144	South	Rocky Mountain birch
SS-01A-1019	10/11/19 13:23	3/11/48 0:00	3.60E+16	6.12	0.08	4589.47	1.68	-2.33	36.42211	-110.06901	2144	South	Rocky Mountain birch
SS-02A-0319	3/11/19 11:31	3/11/48 0:00	3.71E+16	-5.27	0.13	53.60	1.48	-5.96	36.42202	-110.06898	2142	North	Gambel Oak tree
SS-02A-0619	6/15/19 20:17	3/11/48 0:00	3.88E+16	-5.26	0.11	2006.26	1.10	-13.18	36.42202	-110.06898	2142	North	Gambel Oak tree
SS-02A-0818	8/8/18 14:12	3/11/48 0:00	3.92E+16	-8.73	0.14	17.89	1.07	-9.67	36.42202	-110.06898	2142	North	Gambel Oak tree
SS-02A-1019	10/11/19 13:18	3/12/48 0:00	3.72E+16	-9.81	0.20	46.68	1.47	-10.37	36.42202	-110.06898	2143	North	Gambel Oak tree
SS-02A-1218	12/20/18 13:37	3/12/48 0:00	3.93E+16	-5.07	0.13	501.67	1.04	-10.58	36.42202	-110.06898	2142	North	Gambel Oak tree
SS-03A-0319	3/11/19 11:37	3/12/48 0:00	3.76E+16	-2.73	0.15	241.84	1.35	-5.88	36.42194	-110.06899	2142	North	Colorado Pinon Tree
SS-03A-0619	6/15/19 20:22	3/12/48 0:00	3.86E+16	1.96	0.15	9408.91	1.13	-11.47	36.42194	-110.06899	2142	North	Colorado Pinon Tree

SS-03A-0818	8/8/18 14:15	3/12/48 0:00	3.93E+16	-4.51	0.08	26.06	1.07	-5.88	36.42194	-110.06899	2142	North	Colorado Pinon Tree
SS-03A-1019	10/11/19 13:11	3/12/48 0:00	3.85E+16	-7.58	0.07	56.94	1.20	-9.30	36.42194	-110.06899	2143	North	Colorado Pinon Tree
STJ-01-0619	6/15/19 15:53	3/12/48 0:00	3.86E+16	-2.09	0.08	4965.78	1.18	-12.92	36.45793	-110.11542	2194	East	Rocky Mountain Juniper
STJ-01-0818	8/14/18 12:31	3/12/48 0:00	3.94E+16	-11.22	0.19	5.29	1.02	-10.81	36.45793	-110.11542	2194	East	Rocky Mountain Juniper
STJ-01-1019	10/8/19 12:21	3/12/48 0:00	3.83E+16	-7.29	0.20	344.13	1.20	-11.54	36.45793	-110.11542	2194	East	Rocky Mountain Juniper
STJ-01-1218	12/18/18 13:00	3/12/48 0:00	3.97E+16	-8.12	0.11	6.74	1.00	-8.25	36.45793	-110.11542	2194	East	Rocky Mountain Juniper
TL-01-0319	3/9/19 13:19	3/12/48 0:00	3.93E+16	-3.63	0.09	5.30	1.04	-3.17	35.54985	-110.80325	1530	South	Tamarisk shrub
TL-01-0619	6/14/19 9:03	3/12/48 0:00	3.89E+16	-3.05	0.12	30.28	1.07	-4.64	35.54985	-110.80325	1530	South	Tamarisk shrub
TL-01-0818	8/7/18 17:15	3/12/48 0:00	3.81E+16	-3.03	0.32	20.67	1.20	-3.80	35.54985	-110.80325	1530	South	Tamarisk shrub
TL-01-1018	10/6/18 16:00	3/12/48 0:00	3.92E+16	-6.99	0.15	4.09	1.00	-5.52	35.54985	-110.80325	1530	South	Tamarisk shrub
TL-01-1019	10/6/19 13:08	3/12/48 0:00	3.63E+16	-3.71	0.27	63.30	1.58	-4.27	35.54985	-110.80325	1530	South	Tamarisk shrub
TL-01-1218	12/17/18 13:04	3/12/48 0:00	3.45E+16	-6.60	0.14	9.79	1.96	-3.85	35.54985	-110.80325	1530	South	Tamarisk shrub
TL-03-0319	3/9/19 11:01	6/5/48 0:00	3.94E+16	0.60	0.10	6.06	1.03	0.34	35.49939	-110.81172	1527	South	Tamarisk shrub
TL-03-0619	6/14/19 7:33	6/5/48 0:00	3.81E+16	0.65	0.16	369.91	1.27	-3.43	35.49939	-110.81172	1527	South	Tamarisk shrub
TL-03-1019	10/6/19 11:37	6/5/48 0:00	3.65E+16	-2.29	0.06	26.00	1.61	-2.13	35.49939	-110.81172	1527	South	Tamarisk shrub
TL-03-1218	12/17/18 12:02	6/5/48 0:00	3.95E+16	-4.47	0.10	4.67	1.02	-3.90	35.49939	-110.81172	1527	South	Tamarisk shrub
TL-05-0319	3/9/19 11:13	6/5/48 0:00	3.88E+16	-5.71	0.08	138.56	1.13	-8.94	35.49939	-110.81172	1514	South	Greasewood shrub
TL-05-0619	6/14/19 7:55	6/5/48 0:00	3.88E+16	-3.93	0.07	686.73	1.12	-9.60	35.49939	-110.81172	1514	South	Greasewood shrub
TL-05-1018	10/6/18 15:02	6/5/48 0:00	3.94E+16	-7.25	0.09	4.10	1.00	-6.79	35.49939	-110.81172	1514	South	Greasewood shrub
TL-05-1019	10/6/19 12:21	6/5/48 0:00	3.94E+16	-9.82	0.04	16.41	1.00	-11.38	35.49939	-110.81172	1514	South	Greasewood shrub
TL-07-0319	3/9/19 11:37	6/5/48 0:00	3.63E+16	-0.52	0.22	11.03	1.64	0.50	35.43607	-110.84894	1494	South	Tamarisk shrub
TL-07-0619	6/14/19 8:22	6/5/48 0:00	3.77E+16	-2.89	0.18	123.56	1.35	-5.22	35.43607	-110.84894	1494	South	Tamarisk shrub
TL-07-1019	10/6/19 12:42	6/5/48 0:00	3.95E+16	-7.04	0.10	17.29	1.01	-8.60	35.43607	-110.84894	1494	South	Tamarisk shrub
TL-07-1218	12/17/18 12:41	6/5/48 0:00	3.54E+16	-5.79	0.07	14.69	1.85	-4.28	35.43607	-110.84894	1494	South	Tamarisk shrub

WPV-01-0319	3/10/19 8:52	6/5/48 0:00	3.95E+16	-5.48	0.20	4.22	1.01	-4.98	36.39281	-109.92966	2232	South	Gambel Oak tree
WPV-01-1018	10/7/18 12:26	6/5/48 0:00	3.63E+16	-7.17	0.12	127.31	1.65	-8.49	36.39281	-109.92966	2232	South	Gambel Oak tree
WPV-01-1019	10/8/19 18:17	6/5/48 0:00	3.62E+16	-3.15	0.05	514.05	1.62	-6.58	36.39281	-109.92966	2232	South	Gambel Oak tree
WPV-03-0319	3/10/19 10:06	6/5/48 0:00	3.73E+16	-6.09	0.21	48.07	1.41	-7.20	36.38232	-109.94955	2140	North	lodgepole pine (Pinus contorta)
WPV-03-0618	6/5/18 17:37	6/6/48 0:00	3.86E+16	-8.46	0.08	25.27	1.22	-9.59	36.38232	-109.94955	2140	North	lodgepole pine (Pinus contorta)
WPV-03-0619	6/15/19 13:09	6/6/48 0:00	3.77E+16	-9.03	0.11	166.88	1.41	-12.85	36.38232	-109.94955	2140	North	lodgepole pine (Pinus contorta)
WPV-03-1018	10/7/18 12:43	6/6/48 0:00	3.91E+16	13.54	0.16	71937.78	1.01	-10.16	36.38232	-109.94955	2140	North	lodgepole pine (Pinus contorta)
WPV-03-1019	10/8/19 17:53	6/6/48 0:00	3.81E+16	-5.95	0.12	96.38	1.32	-9.33	36.38232	-109.94955	2140	North	lodgepole pine (Pinus contorta)
WPV-03-1218	12/18/18 12:58	6/6/48 0:00	3.97E+16	-8.09	0.17	6.03	1.00	-7.94	36.38232	-109.94955	2140	North	lodgepole pine (Pinus contorta)
WR-01-0619	6/20/19 10:48	6/6/48 0:00	3.99E+16	-9.57	0.11	6.15	1.00	-9.38	36.30148	-110.13306	1969	South	Tamarisk shrub
WR-01-1019	10/10/19 16:17	6/6/48 0:00	3.65E+16	-3.43	0.16	227.87	1.63	-7.06	36.30148	-110.13306	1969	South	Tamarisk shrub
WR-01-1218	12/18/18 8:13	6/6/48 0:00	3.94E+16	-3.54	0.07	145.01	1.08	-7.57	36.30148	-110.13306	1969	South	Tamarisk shrub
WRV-01-0319	3/10/19 11:57	6/6/48 0:00	4.00E+16	-7.76	0.11	4.93	1.00	-7.56	36.35349	-109.83324	2442	North	lodgepole pine (Pinus contorta)
WRV-01-0619-12	6/15/19 12:46	6/6/48 0:00	3.81E+16	-9.97	0.12	167.32	1.34	-14.00	36.35349	-109.83324	2442	North	lodgepole pine (Pinus contorta)
WRV-01-0619-9	6/15/19 9:04	6/6/48 0:00	3.94E+16	-9.44	0.15	573.45	1.09	-15.59	36.35349	-109.83324	2442	North	lodgepole pine (Pinus contorta)
WRV-01-0818	8/9/18 16:17	6/6/48 0:00	3.95E+16	-7.46	0.10	9.53	1.07	-7.34	36.35349	-109.83324	2442	North	lodgepole pine (Pinus contorta)
WRV-01-1018	10/7/18 11:09	6/6/48 0:00	3.85E+16	-3.20	0.08	108.58	1.29	-6.77	36.35349	-109.83324	2442	North	lodgepole pine (Pinus contorta)
WRV-01-1019	10/11/19 9:59	6/6/48 0:00	3.81E+16	-10.56	0.17	24.52	1.35	-10.87	36.35349	-109.83324	2442	North	lodgepole pine (Pinus contorta)
WRV-01-1218	12/20/18 10:12	6/6/48 0:00	3.93E+16	7.74	0.08	14617.67	1.02	-7.51	36.35349	-109.83324	2442	North	lodgepole pine (Pinus contorta)
WRV-05-0319	3/10/19 13:06	6/6/48 0:00	3.73E+16	-1.51	0.05	75.18	1.47	-4.12	36.34884	-109.84081	2386	North	Rocky Mountain birch
WRV-05-0619	6/15/19 9:58	6/7/48 0:00	3.94E+16	-8.26	0.03	82.78	1.07	-11.32	36.34884	-109.84081	2386	North	Rocky Mountain birch
WRV-05-1019	10/11/19 10:43	6/7/48 0:00	3.75E+16	-10.48	0.11	22.09	1.44	-11.64	36.34884	-109.84081	2386	North	Rocky Mountain birch
WRV-05-1218	12/20/18 10:52	6/7/48 0:00	3.85E+16	-1.86	0.08	56.71	1.29	-4.13	36.34884	-109.84081	2386	North	Rocky Mountain birch

WRV-07-0619	6/15/19 10:50	6/7/48 0:00	3.82E+16	-8.91	0.19	122.20	1.30	-11.95	36.34132	-109.88338	2195	North	Rocky Mountain birch
WRV-07-0818	8/9/18 17:24	6/7/48 0:00	3.96E+16	-6.29	0.16	74.65	1.04	-9.22	36.34132	-109.88338	2195	North	Rocky Mountain birch
WRV-07-1018	10/7/18 11:54	6/7/48 0:00	3.70E+16	-3.64	0.21	258.37	1.52	-7.05	36.34132	-109.88338	2195	North	Rocky Mountain birch
WRV-07-1019	10/11/19 11:30	6/7/48 0:00	3.72E+16	-9.63	0.11	55.46	1.50	-11.41	36.34132	-109.88338	2195	North	Rocky Mountain birch
WRV-07-1218	12/20/18 11:16	6/7/48 0:00	3.74E+16	-3.74	0.20	206.75	1.44	-7.05	36.34132	-109.88338	2195	North	Rocky Mountain birch
WRV-09-0319	3/10/19 13:35	6/7/48 0:00	3.69E+16	-5.46	0.15	59.89	1.56	-7.17	36.34134	-109.88374	2205	North	Gambel Oak tree
WRV-09-0619	6/15/19 10:37	6/7/48 0:00	3.87E+16	-7.85	0.11	522.37	1.16	-13.18	36.34134	-109.88374	2205	North	Gambel Oak tree
WRV-09-1018	10/7/18 11:53	6/7/48 0:00	3.88E+16	-5.77	0.08	251.13	1.16	-10.04	36.34134	-109.88374	2205	North	Gambel Oak tree
WRV-09-1019	10/11/19 11:10	6/7/48 0:00	3.49E+16	-4.26	0.39	300.70	1.88	-7.02	36.34134	-109.88374	2205	North	Gambel Oak tree
WRV-01-0319	3/10/19 11:57	6/7/48 0:00	3.97E+16	-7.49	0.19	7.81	1.00	-8.48	36.35349	-109.83324	2442	North	lodgepole pine (Pinus contorta)
WRV-01-0818	8/9/18 16:17	6/7/48 0:00	3.94E+16	-7.04	0.04	9.86	1.07	-8.32	36.35349	-109.83324	2442	North	lodgepole pine (Pinus contorta)
WRV-01-1019	10/11/19 9:59	6/7/48 0:00	3.79E+16	-9.98	0.15	22.00	1.35	-11.37	36.35349	-109.83324	2442	North	lodgepole pine (Pinus contorta)

APPENDIX C: GROUNDWATER DATES DATA

Name: Slick
Batch ID: 5406

Chemistry Blanks

Atomic Mass of Cl: 35.4527

Submitter Name	Nuclide Id	Sample Id	Aliquot Id	User Identification	Sample Mass (g)	Native Chlorine (mg)	Cl Carrier (mg)	Average Current (nA)	Interference (Counts/Sec)	^{36}Cl Ratio ($x10^{-15}$)	^{36}Cl Std Dev ($x10^{-15}$)	Use? 0 or 1	Atoms ^{36}Cl per mg of Cl Carrier	Std Dev	Total Atoms ^{36}Cl Added by Process	Std Dev
Slick	5	202101294	A	Carrier Dir PPT 5406			1.732	28655	1.6	2.933	0.628		49,826	10,661		
Slick	5	202101293	A	Cblk5406-1			2.024	29017	2.9	4.458	0.737	1	75,733	12,523	52,437	33,287
												0				
												0				
												0				
												0				
												0				
												1	75,733	12,523	52,437	33,287
												Difference per mg of Cl Carrier:	25,908	16,446		

Submitter Name	Nuclide Id	Sample Id	Aliquot Id	User Identification	Sample Mass (g)	Native Chlorine (mg)	Cl Carrier (mg)	Average Current (nA)	Interference (Counts/Sec)	^{36}Cl Ratio ($x10^{-15}$)	^{36}Cl Std Dev ($x10^{-15}$)	Total ^{36}Cl Atoms	Std Dev	Carrier/Process Corrected Total ^{36}Cl Atoms	Carrier/Process Corrected Std Dev	Native ^{36}Cl Ratio ($x10^{-15}$)	Std Dev	Relative Uncertainty (%)	Uncertainty in the AMS Measurement (%)
Slick	5	202101285	A	SPR-OS3	407.257			31168	2.6	742.0	16.7	0	0	-52,437	33,287	#DIV/0!	#DIV/0!	#DIV/0!	2.3
Slick	5	202101286	A	SPR-PD	207.186			35802	2.9	1067	28	0	0	-52,437	33,287	#DIV/0!	#DIV/0!	#DIV/0!	2.6
Slick	5	202101287	A	SPR-SS1	205.730			39171	3.7	995.9	25.8	0	0	-52,437	33,287	#DIV/0!	#DIV/0!	#DIV/0!	2.6
Slick	5	202101288	A	SPR-AWS	924.836			30922	6.7	5403	133	0	0	-52,437	33,287	#DIV/0!	#DIV/0!	#DIV/0!	2.5
Slick	5	202101289	A	WM-308-1	204.831			37220	2.5	326.2	9.6	0	0	-52,437	33,287	#DIV/0!	#DIV/0!	#DIV/0!	2.9
Slick	5	202101290	A	WM-311-4	843.052			38512	3.9	1647	42	0	0	-52,437	33,287	#DIV/0!	#DIV/0!	#DIV/0!	2.5
Slick	5	202101291	A	WM-4T-399	605.443			38863	2.9	784.8	18.5	0	0	-52,437	33,287	#DIV/0!	#DIV/0!	#DIV/0!	2.4
Slick	5	202101292	A	WM-4T-500	604.052			33655	3.2	1225	28	0	0	-52,437	33,287	#DIV/0!	#DIV/0!	#DIV/0!	2.3